THESIS WORK

Master of Science in Energy and Environment

Instituto Tecnológico de Buenos Aires - Karlsruhe Institute of Technology

FEASIBILITY STUDY OF A HYDROGEN FUELED INTERNAL COMBUSTION HYBRID BUS OPERATING UNDER REAL TRAFFIC URBAN CONDITIONS IN BUENOS AIRES, ARGENTINA

Sven Britz
Mechanical Engineer (KIT)

Tutor
Dr. Pedro Orbaiz (ITBA)

Examiners
Dr. Roberto Vieytes (INLAB S.A. – ITBA)
Lic. Ricardo Lauretta (ITBA)
Dra. Ing. Cecilia Smoglie (ITBA)
Prof. Dr. Ing. Martin Gabi (KIT)

Buenos Aires
18/12/2018

Abstract

This thesis evaluates the technical, economic and environmental performance of a hydrogen fueled hybrid bus, which uses an internal combustion engine as a power unit. Results are compared to those of a conventional diesel bus and to those of two commercially available hydrogen fuel cell buses. The performance of the different vehicles, under real driving conditions, is evaluated using validated models of these on the Autonomie simulation platform. On the other hand, the life-cycle GHG emissions of the buses are estimated with hydrogen being produced from different primary sources. Whilst the first scenario assumes that hydrogen is produced from natural gas via steam methane reforming, the other three assume electrolytic production using different electricity production mixes. Finally the total cost of ownership of each hybrid bus is calculated and compared to that of the conventional bus. Results show that all hydrogen buses have a considerable lower energy consumption than that of the conventional vehicle. This is manly due to the use of the hybrid powertrain architecture. When comparing the different hydrogen buses, as expected, the fuel cell vehicles result in a higher efficiency than the internal combustion engine vehicles, but in a considerable higher cost, making the use of internal combustion engines a more cost effective way to reduce GHG emissions. The life cycle emission analysis shows that the environmental performance of all hydrogen vehicles is highly dependent on the carbon intensity of the hydrogen production. Overall, whilst fuel cells are more efficient than ICEs, the considerable lower cost of ICEs makes the H2ICE hybrid bus a more cost effective way of reducing GHG emissions.

Abstract

In dieser Arbeit wird ein, mit einem Wasserstoff-Verbrennungsmotor angetriebener, Hybrid-Bus hinsichtilich technischer, ökologischer und finanzieller Aspekte untersucht. Als Referenzmodell dient ein konventioneller Disel-Bus sowie zwei kommerziell erhältliche Brennstoffzellen Hybrid-Buse. Zum Leistungsvergleich, unter realen Fahrbedingungen, werden die Buse in der Simulationssoftare Autonomie modeliert, validiert und verglichen. Desweiteren werden, um den ökologischen Fußabdruck der Buse zu ermitteln, die Treibhausgase der einzelnen Buse über deren komplette Lebensdauer ermittelt. Dazu werden für die Wasserstoffproduktion verschiedene Scenarien untersucht: Wasserstoffproduktion durch Steam-Methane-Reforming und Wasserstoffproduktion durch Electrolyse mit verschiedenen Scenarien der Elektrisitätsproduktion. Letztlich werden die Gesamtbetriebskosten der Buse ermittelt und mit denen des Dieselbuses verglichen. Die Ergebnisse zeigen, dass alle Wasserstoffbusse, auf Gurnd der Hybridisierung, im Vergleich zum Dieselbus eine erhebliche Reduzierung des Kraftstoffverbrauchs vorweisen können. Wie erwartet zeigt der Vergleich der Wasserstoffbuse, dass die Brenstoffzellen-Buse einen höheren Wirkungsgrad erzielen als die VM-Wasserstoffbuse. Allerdings übersteigen die Kosten der Brennstoffzellen die Kosten der Verbrennungsmotoren bei weitem, weshalb der VM-Wasserstoffbus die deutlich kostengünstigere Variante zur Treibhausgasreduzierung darstellt. Desweiteren hängt der ökologische Fußabdruck der Wasserstoffbuse stark von der Wasserstoffherstellung abhängt. Allgemein kann festgehalten werden, dass die Brennstoffzellenbuse effizienter, die VM-Wasserstoffbuse aber die deutlich kostengünstigere Variante zur Treibhausgasreduzierung darstellen.

Abstract

En esta tesis se analiza el rendimiento técnico, económico y ambiental de un bus híbrido alimentado a hidrógeno, que utiliza un motor de combustión interna (MCI) como unidad de potencia. Los resultados se comparan con los de un bus diesel convencional y con los de dos buses de celdas de combustible de hidrógeno disponibles comercialmente. El rendimiento de los mismos es evaluado con modelos computacionales utilizando la plataforma de simulación Autonomie. Dichos modelos son validados con información disponible en la literatura con ciclos de manejo reales. Por otro lado, las emisiones de GEI (Gases de Efecto Invernadero) del ciclo de vida de los buses son estimadas y se proponen diferentes escenarios según el origen del hidrógeno utilizado como combustible. Se analizan cuatro escenarios: en el primero se asume que el hidrógeno es producido mediante el reformado de vapor-metano y en los tres restantes se asume que es producido mediante electrólisis de agua utilizando energía eléctrica de la red con diferentes intensidades de carbono. Finalmente se calcula el costo de vida total de cada bus hibrido y se lo compara con el del bus convencional. Los resultados muestran que los buses a hidrógeno analizados tienen un consumo de energía sensiblemente menor que el de un bus convencional; esto se debe principalmente a la presencia de la arquitectura híbrida. Los buses híbridos con celda de combustible presentan una eficiencia global mayor que la del bus con MCI pero con un costo de vida total considerablemente mayor. Este resultado presenta al uso de MCI a hidrógeno como una alternativa económica para reducir los GEI. El análisis medioambiental muestra que el desempeño de los buses a hidrógeno es altamente dependiente de la intensidad de carbono de la red eléctrica considerada. Como conclusión, si bien las celdas de combustible son más eficientes que los MCI, el costo considerablemente menor de los MCI hace que el bus híbrido H2ICE sea una forma más económica de reducir las emisiones de GEI.

Contents

List of Figures

List of Tables

Nomenclature

Roman Symbols

$(\frac{F}{A})$	Fuel-Air Ratio
$\Delta_R H$	Enthalpie of Reaction
λ	Lambda
ϕ	Fuel-Air Equivalence Ratio
ADR	Assembly Disposal and Recycling
$BADC$	Buenos Aires Driving Cycle
$BCDC$	Braunschweig City Driving Cycle
C_8H_{18}	Iso-Octane
C_t	Net Cash Inflow during the Perido t
CB	Conventional Bus
CH_4	Methane
CO_2	Carbon Dioxide
E	Energy
e^-	Electron
E^{xx}	Electrode Potential
EEE	Embedded Energy and Emissions
EOL	End of Lifetime

ESS	Energy Storage System
FC	Fuel Cell
$FCHB$	Fuel Cell Hybrid Bus
$GREET$	Greenhouse Gases Regulated Emissions and Energy use in Transportation
GWP	Global Warming Potential
$H2ICE$	Hydrogen Fueled Internal Combustion Engine
$H2ICE-Li$	Hydrogen fueled Internal Combustion Engine with Li-Ion Batteries
$H2ICE-ultracaps$	Hydrogen fueled Internal Combustion Engine with ultra-capacitors
H^+	Hydrogen Proton
H_2	Hydrogen
H_2O	Water
H_3O^+	Hydronium
H_u	Lower Heating Value
HC	Hydrocarbon
ICE	Internal Combustion Engine
LCI	Life Cycle Inventory
m	Mass
NPV	Net Present Value
O_2	Oxygen
OH^-	Hydroxide
P	Power
PM_{10}	Particles between 2.5 and 10 Microns

$PM_{2.5}$	Ultrafine Particles
r	Discount Rate
SO_X	Sulfur Dioxide
SOC	State of Charge
t	Time
VMA	Vehicle Manufacture and Assembly
$WMATA$	Driving Cycle of Washington D.C.
CO	Carbon Monoxide
DOD	Depth of discharge
PEMFC	Polymere Electrolyte Membrane Fuel Cell
TCO	Total cost of ownership
TTW	Tank to Wheel
WTT	Well to Tank
WTW	Well to Wheel

Chapter 1

Introduction

1.1 Introduction and Thesis Context

The scientific comity is set on the fact that greenhouse gas emissions (GHG) have a direct impact on global warming. Figure 1.0.1 and 1.0.2 show the increasing GHG emissions and the average temperature anomaly´between 1970 and 2012. It can be clearly seen that with the start of the increase of the GHG emissions also the average temperature started to increase [48]. Especially in the last few years the increase of the temperature became even stronger.

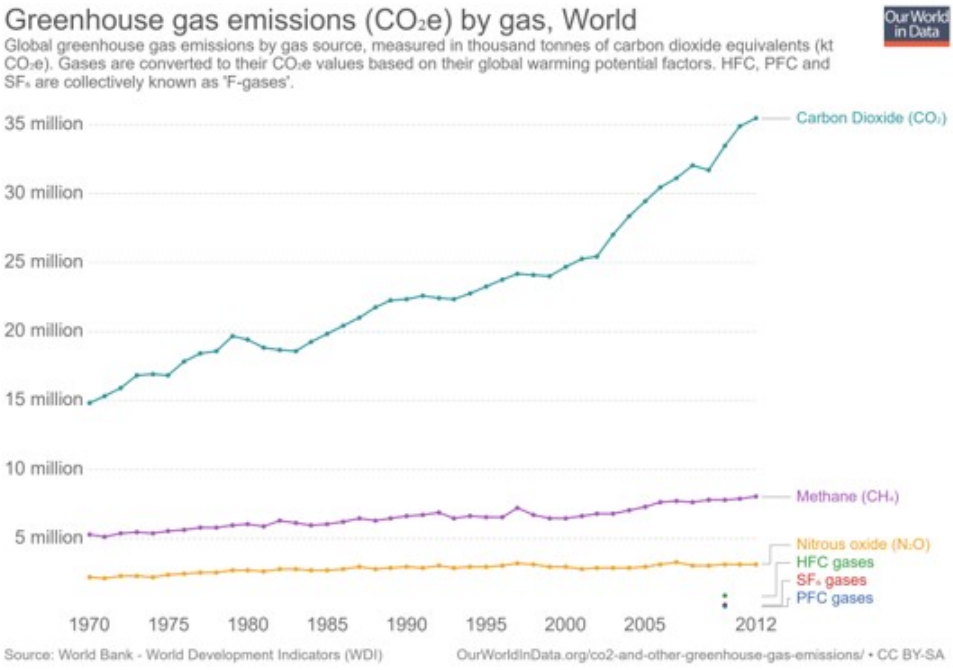

Figure 1.1.1: World greenhouse gas emissions CO_2 eq. [48]

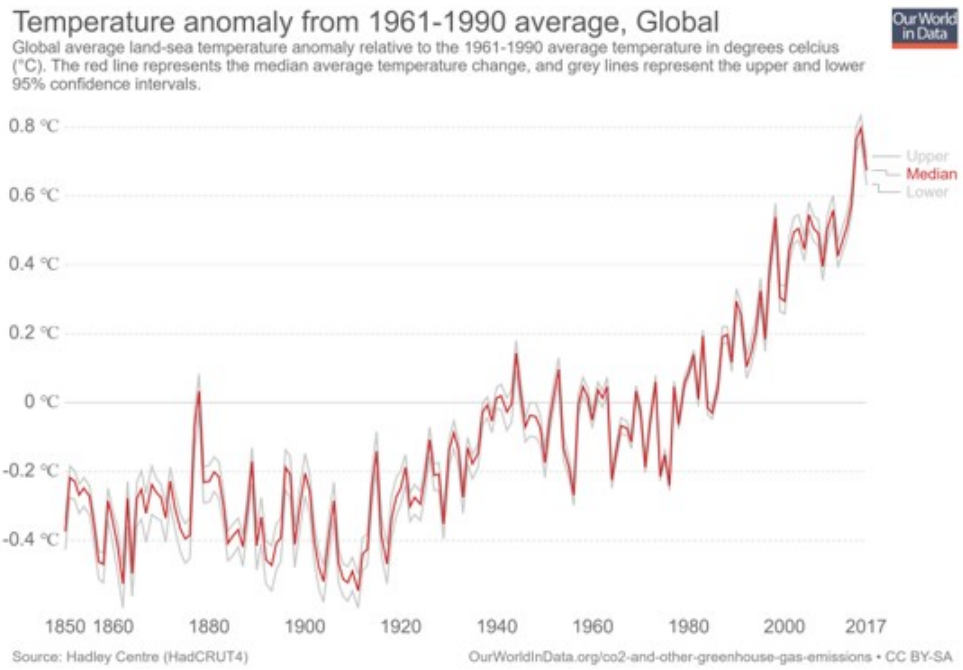

Figure 1.1.2: Global average land-sea temperature anomaly relative to the 1961-1990 average temperature [48]

The greenhouse gases heat up the earth by holding back the outgoing longwave thermal radiation. The only way to contain the effect of global warming is to reduce the concentration of greenhouse gases in the atmosphere. GHG emissions rose dramatically since the industrial revolution. As can be seen in Figure 1.0.3, all sectors of the economy contribute to the problem, with transport of people and good accounting for 14% of global GHG emissions.

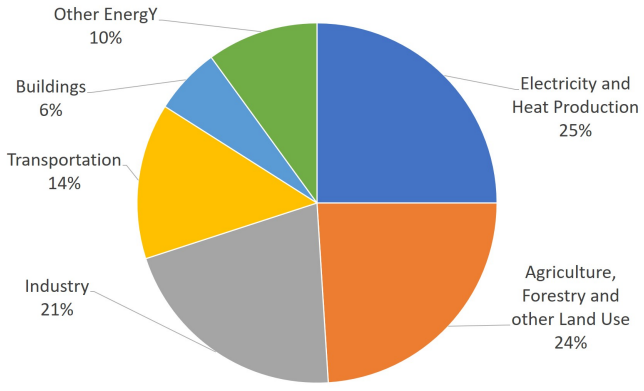

Figure 1.1.3: GHG Emissions by economic sectors [27]

A big part of the GHG emissions in the transport sector are produced by trucks and buses, specially in developing countries in which buses are the main public transportation medium.Within the energy compilation the transport sector is responsible for almost 30% of the energy consumption [14] (Figure 1.0.4). As can be seen, most of the transportation sector is powered by diesel and gasoline fueled applications such as conventional diesel buses for public transportation. In 2016 the bus fleet of Buenos Aires Capital City was liable for over 5% of the diesel consumption of the entire country [14, 15].

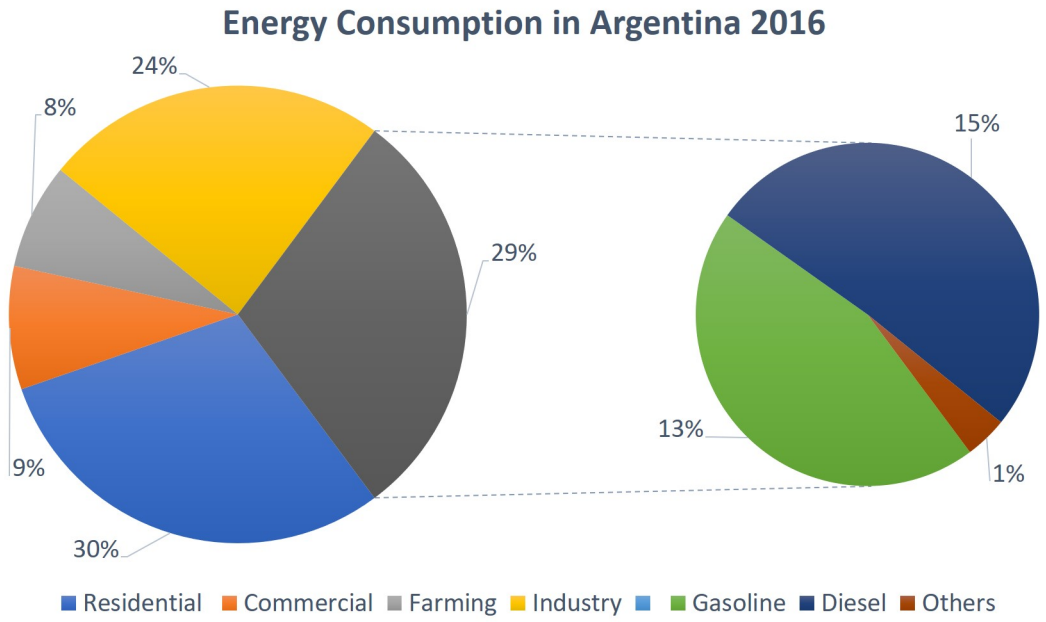

Figure 1.1.4: Energy consumption in Argentina by sectors [14]

Another big problem of urban diesel buses is that they produce local pollutant emissions during operation which directly affects the air quality of the city. These include unburned carbons (HC), nitro oxides (NO_X) and particulate matter (PM). NO_X is a highly toxic and odorless gas that plays an important role in the tumorigenesis of lung cancer. In a stationary atmosphere the HCs and oxygen (O_2) produce, under the influence of solar radiation, the toxic and eye irritating photo chemical smog, visible as a brown haze and known as 'Los Angeles Smog' [24, 33].

Further, noise levels of urban diesel buses is around 80-85dB and increases, as vehicles age. This noise levels affects the well-being of the people who live within the big cities. The bus fleet in Buenos Aires counts 9,200 Buses in the federal district and over 18,000 vehicles

in the metropolitan region. The transport system operates 24 hours a day. Whilst the buses providing a good transportation service, emissions and noise have a strong impact on the life quality of the city population.

Based on the reasons above it is necessary to look out for alternatives that allow to maintain the quality of the service whilst reducing the environmental impact of the system. Extending research has been done regarding alternative technology buses such as electric and hybrid buses [9, 19, 29, 40, 46, 56]. Also for private use electric vehicles becoming more common because of their zero direct emissions. However, electric vehicles have still range problems what limits their use, especially in public transportation. When investigating hydrogen fueled vehicles, the fuel cell system is the most common technology. However, the reliability of the powertrain, essential in public transportation, of fuel cell systems is much lower compared to internal combustion engines. Furthermore are the costs of fuel cell systems and their maintenance still very high. Therefore, in this work a hydrogen fueled internal combustion engine hybrid bus will be determined to see if this technology can be, with its cost efficiency and reliability, a seriousness alternative to other zero emission vehicles.

In the following chapter a literature review gives an overview over the in this work used hydrogen characteristics and hydrogen to power technologies.

Chapter 2

Literature Review

In order to understand the technical, economic and environmental feasibility of H_2 fueled buses, this chapter reviews the technical foundations of hydrogen as fuel for both Fuel cell and internal combustion engine applications. First, different sources of hydrogen production are evaluated and for each source the production process is described and explained. As Fuel Cell hybrid buses work as zero direct emission reference model, a short review of Fuel Cell and their working process is given. Then the hydrogen properties, which are important for the use in hydrogen fueled combustion engines, are discussed in detail. Finally an overview of hybrid vehicles and electrical energy storage systems is done.

2.1 Hydrogen

50 million tons of hydrogen are produced worldwide, per year. 40% of which is produced in industrial processes such as the production of chlorine, the refining of crude oil or the production of ethene or methanol. The remaining 60% is produced mainly from fossil hydrocarbons as shown in figure 2.1.1 [32].

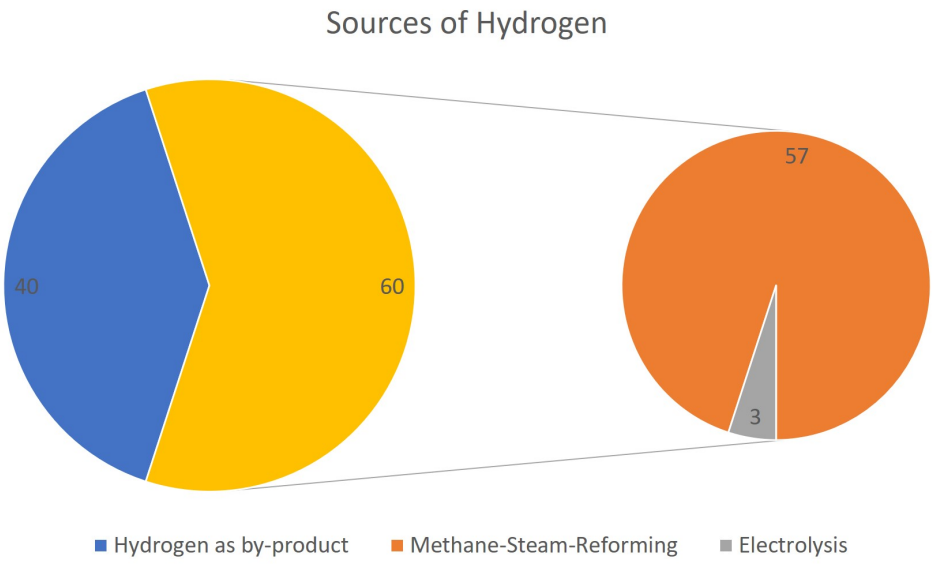

Figure 2.1.1: Sources of hydrogen. [32]

Only 5% of the hydrogen is produced using electrolysis as production method. The most used production process is Steam-Methane-Reforming (SMR). There are some other sources of hydrogen like gasification of biomass, biological and photo chemical processes or direct thermal fission. However, these methods are still areas under investigation and not used in big scales. To the present, electrolysis is the only way to produce emission-free hydrogen, but only if electricity is produced from renewable energy sources like wind or solar power [32, 49]. Next, the two main production processes are explained in detail.

2.1.1 Steam-Methane-Reforming

Figure 2.1.2 shows the scheme of a Steam-Methane-Reforming system. In this process hydrogen is produced in an endothermic catalytic transformation from hydrocarbons and water vapor. The process occurs under high temperatures, normally ranging between 700 and 900 degree Celsius and high pressure, ranging between 20 and 40 to up to 80 bar. The main components are a steam-methane-reformer, heat transfer blocks, expansion valves and a hydrogen separation membrane. Catalysts are used to speed up the reaction. These are mainly nickel based. In the furnaces, the following two reactions occur [32, 49]:

$$CH_4 + H_2O \rightarrow CO + 3H_2 \; \Delta_R H = 206 \frac{kJ}{mol}$$

$$CH_4 + 2H_2O \rightarrow CO_2 + 4H_2 \; \Delta_R H = 165 \frac{kJ}{mol}$$

The CO leaves the reformer at 850 degree Celsius. After that it gets dismantled in another reaction:

$$CO + H_2O \rightarrow CO_2 + H_2 \; \Delta_R H = -41 \frac{kJ}{mol}$$

Big industrial steam methane reformers have a capacity of 100,000$\frac{m^3}{h}$ and an efficiency between 75 and 80%. For the production of 1m^3pure hydrogen an amount of 0.45$m^3$of methane is necessary [32].

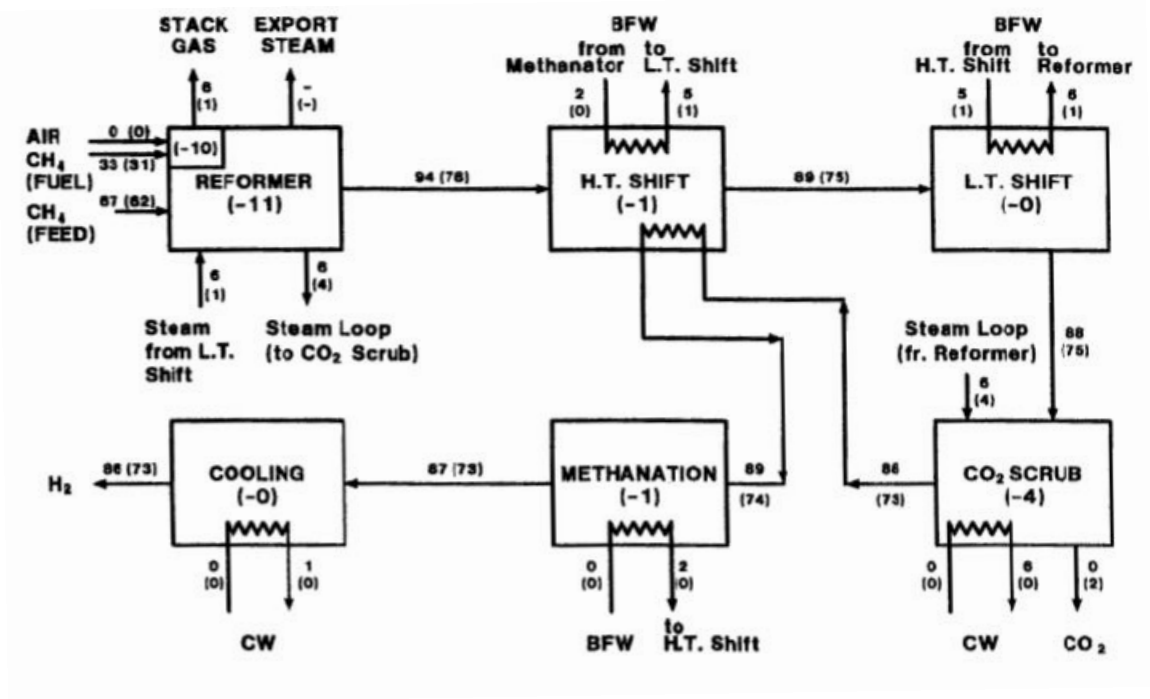

Figure 2.1.2: SMR [49]

Methane is mixed with steam, super heated by burning methane, in the reformer. In the High-temperature shift 94% of the CO in the gas is shifted. In the Low-temperature shift 83% of the remaining CO in the gas is shifted. After that, the gas is compressed and the CO_2 is removed. In the cooler the water is removed and the outcome is 97% pure hydrogen [49]. Since this purity is insufficient to use the hydrogen in fuel cells, it has to be cleaned before it can be used. Also, because of the use of methane, the production process is not emission free. However it is the cheapest and therefore most used process to produce hydrogen.

2.1.2 Electrolysis

In the electrolysis, electrical energy is transformed in chemical energy. Figure 2.1.3 shows the electrolysis process [32]. An electrolyzer consists of an anode and a cathode separated by an electrolyte (salt water solution). The electrodes are connected with an external power supply. The negatively biased cathode gives e^- into the electrolyte. At a certain voltage the water dissociates to H_3O^+ and OH^-. The H_3O^+-Ions take the free e^- and give up a H^+. The H^+-Ions connect to hydrogen gas and the OH^--Ions travel through the electrolyte to the positively biased electrode. There, the Ions give up an electron to the anode and produce H_2O and O_2.

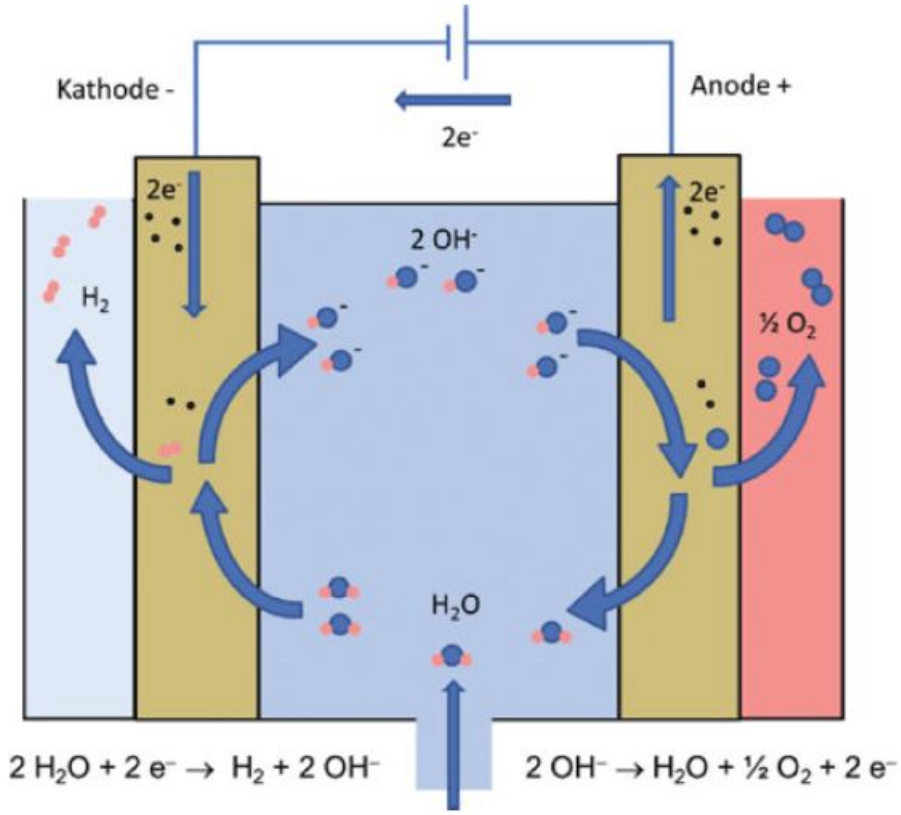

Figure 2.1.3: Electrolysis [32]

The amount of gases produced per unit time is directly related to the current that passes through the electrochemical cell. The water always includes a certain number of OH^--Ions and H_3O^+-Ions. To increase the electrical conductivity acids or bases are added to the water.

At the cathode the following reactions occur:

$$4H_2O \rightarrow 2H_3O^+ + 2OH^-$$

$$2H_3O^+ + 2e^- \rightarrow H_2 + 2H_2O$$

At the anode the following reactions occur:

$$2OH^- \rightarrow H_2O + \tfrac{1}{2}O_2 + 2e^-$$

The chemical overall reaction of the process is:

$$H_2O(l) \rightarrow H_2(g) + \tfrac{1}{2}O_2(g)\ \Delta_R H = 286\tfrac{kJ}{mol}$$

As can be seen in the overall reaction, a high energy input is necessary to produce hydrogen from water. To produce 1 kmol hydrogen out of 1 kmol water theoretically an energy input of 286 MJ is required.

Electrolysis can achieve an efficiency of 85% and produce highly pure hydrogen [20, 32]. Another big advantage of the electrolysis is that the production process can be completely emission free and is not dependent on fossil fuels. But to achieve a emission free hydrogen production, electricity from renewable energies has to be used. However, the high energy demand of the electrolysis creates high production costs.

2.2 Hydrogen to Power

There are two possibilities to produce power from hydrogen. The most common technology is the cold combustion, using a fuel cell. However, the maintenance costs are still very high. The second one is the hydrogen fueled internal combustion engine, which could combine the well known and cheap internal combustion engine with the clean combustion of hydrogen. In the following paragraphs a short description of fuel cells is given before the characteristics of a hydrogen fueled internal combustion engine are explained in detail.

2.2.1 Fuel Cell

Because the H2ICE hybrid buses are compared with fuel cell hybrid buses, follows a short overview over the working process of fuel cells.

The principle working process of a fuel cell is always the same, but can be achieved with several types of electrolytes and designs. To explain the principle working process, a single cell of polymer electrolyte membrane fuel cell (PEMFC) is shown in figure 2.2.1. The

hydrogen goes trough the flow channel and diffuses trough the gas diffusion layer to the anode. Hydrogen ionizes at the anode to hydrogen protons. The hydrogen ionization reaction is shown in the following formula:

$$H_2 \rightarrow 2H^+ + 2e^-, E^{02} = 0V \text{ [32, 35]}$$

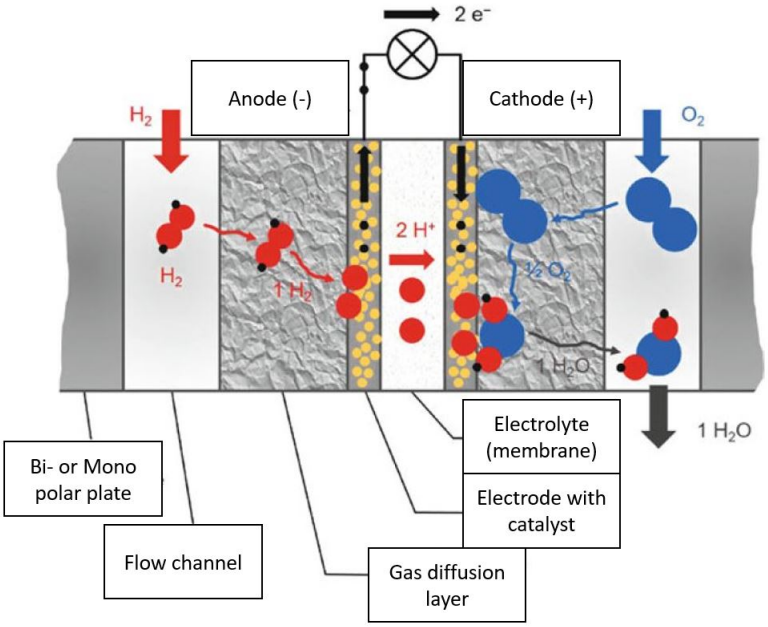

Figure 2.2.1: PEM-Fuel Cell [32]

The electrolyte is conductive for the H^+protons but isolates the e^-electrons. The protons are able to pass the membrane and travel to the cathode. Because of the potential difference, the electrons flow trough the external circuit to the anode. This flowing current can be used to produce electrical power.

On the other half of the fuel cell, oxygen flows through the flow channel and diffuses trough the gas diffusion layer to the cathode. At the cathode the oxygen takes the two electrons and reacts with the H^+protons. The oxygen reduction reaction (ORR) is:

$$\frac{1}{2}O_2 + 2H^+ + 2e^- \rightarrow H_2O(l), E^{01} = 1.229V \text{ [32]}$$

The complete reaction can be written as:

$$H_2 + \frac{1}{2}O_2 \rightarrow H_2O(l), E^0 = E^{01} - E^{02} = 1.229V \text{[32]}$$

How the electrode potentials are determined is further explained in literature [35].

PEMFC are already used in different vehicles and also in public transportation as can be seen in several researches [1, 7, 21, 26, 31, 42, 43].

Compared to the H2ICE engine, fuel cells can reach a higher efficiency but are still subject of development and the reliability of highly developed ICE can not be achieved. Another disadvantage is the high costs of fuel cell systems as well as of the maintenance. Therefore the hydrogen fueled internal combustion engine could be a good alternative, because it is an well known and cheap technology.

2.2.2 Hydrogen Fueled Internal Combustion Engine

To understand the differences between the combustion of fossil fuels and the combustion of hydrogen, it is necessary to take a look at the properties of hydrogen and to compare them with those of fossil fuels. The table 2.1 lists some properties of hydrogen compared with those of methane and iso-octane, which are representing a gaseous and a liquid fossil fuels.

Property	Hydrogen	Methane	Iso-octane
Molecular weight [$\frac{g}{mol}$]	2.016	16.043	114.236
Density [$\frac{kg}{m^3}$]	0.08	0.65	692
Mass diffusivity in air [$\frac{cm^2}{s}$]	0.61	0.16	~0.07
Minimum ignition energy [mJ]	0.02	0.28	0.28
Flammability limits [λ]	10-0.14	2-0.6	1.51-0.26
Flammability limits [φ]	0.1-7.1	0.5-1.67	0.66-3.85
Lower heating value [$\frac{MJ}{kg}$]	120	50	44.3
Stoichiometric air-to-fuel ratio [$\frac{kg}{kg}$]	34.2	17.1	15.0
Stoichiometric air-to-fuel ratio [$\frac{kmol}{kmol}$]	2.387	9.547	59.666

Table 2.1: Properties of hydrogen, methane and iso-octane at 300 K and 1 atm [54]

There are some advantages in the combustion of hydrogen. The high mass diffusivity in air (0.61 $\frac{cm^2}{s}$) compared to iso-octane (~0.07 $\frac{cm^2}{s}$) guaranties a fast and homogeneous H_2-air mixture formation. This is a prerequisite to avoid both rich and lean zones in the fuel-air mixture in order to guarantee a complete combustion.

A rich mixture is defined as a mixture in which not enough oxygen is available to burn all the fuel. In contrast, lean mixtures are those in which more oxygen is available than needed for the combustion of the fuel. If a mixture includes exactly the amount of oxygen that is

necessary to burn all the fuel, it is called a stoichiometric mixture. Because the stoichiometric fuel-air ratio depends on fuel composition, another parameter is defined. The fuel-air equivalence ratio ϕ is the ratio between actual fuel-air ratio and the stoichiometric fuel-air ratio [28, 32].

$$\phi = \frac{(\frac{F}{A})_{actual}}{(\frac{F}{A})_{st}}, \lambda = \phi^{-1} = \frac{(\frac{A}{F})_{actual}}{(\frac{A}{F})_{st}} \text{ [24]}$$

The flammability range of $0.14<\lambda<10$ is very wide compared to those of methane and iso-octane. This allows burning hydrogen in very rich or very lean compositions.

Some properties have to be looked at as mixture properties of hydrogen and air. To explain the most important mixture properties, table 2.2 lists some properties of hydrogen under different fuel-air-ratios compared with an iso-octane-air-mixture.

Property	$H_2 - air$ $\lambda = 1$	$H_2 - air$ $\lambda = 4$	$C_8H_{18} - air$ $\lambda = 1$
Volume fraction fuel [%]	29.5	9.5	1.65
Mixture density $[\frac{kg}{m^3}]$	0.850	1.068	1.229
Kinematic viscosity $[\frac{mm^2}{s}]$	21.6	17.4	15.2
Autoignition temperature [K]	858[a]	>858[a]	690[a]
Adiabatic flame temperature [K]	2390	1061	2276
Thermal conductivity $[10^{-2}\frac{W}{mK}]$	4.97	3.17	2.36
Thermal diffusivity $[\frac{mm^2}{s}]$	42.1	26.8	18.3
Ratio of specific heats	1.401	1.400	1.389
Speed of sound $[\frac{m}{s}]$	408.6	364.3	334.0
Air-to-fuel ratio $[\frac{kg}{kg}]$	34.2	136.6	15.1
Mole ratio before/after combustion	0.86	0.95	1.07
Laminar burning velocity ~360K $[\frac{cm}{s}]$	290	12	45
Gravimetric energy content $[\frac{kJ}{kg}]$	3758	959	3013
Volumetric energy content $[\frac{kJ}{m^3}]$	3189	1024	3704

Table 2.2: Mixture properties of hydrogen-air and iso-octane-air at 300 K and 1 atm [54]

The laminar burning velocity of hydrogen (290 $\frac{cm}{s}$) compared to that of iso-octane (45 $\frac{cm}{s}$) generates a faster heat release. Also, the adiabatic flame temperature is higher than the one of iso-octane, for the same λ. Even though hydrogen has a very high heat value the volumetric

energy content of a λ=1 hydrogen-air mixture is 14% smaller than a C_8H_{18}-air mixture of $\lambda = 1$ because of the very low density [47].

However, running the H2ICE under $\lambda = 1$ conditions generates some problems which can be explained with a closer look at the ignition energy and the adiabatic flame temperature .

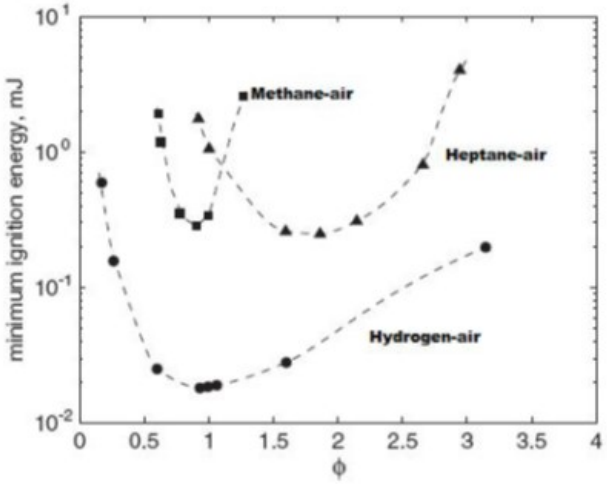

Figure 2.2.2: Minimum ignition energy of Hydrogen-air, Methane-air and Heptane-air [54]

The minimum ignition energy of hydrogen-air in λ=1 operation is very low as can be seen in figure 2.2.2. This can lead to pre-ignition problems. Hot combustion chamber parts like the valves can ignite the hydrogen-air mixture before the spark discharge. The pre-ignition results in a higher heat release and that leads to faster pressure increase. This, in turn, advance the start of combustion further and leads to a runaway effect. The higher peak cylinder pressure can damage the engine [17, 54]. Figure 2.2.2 also shows that the minimum ignition energy for high λ's still is comparable to the minimum ignition energy of methane or iso-octane mixtures. This allows burning very lean hydrogen-air mixtures with common ignitors.

The mentioned high laminar burning velocity and the very fast heat release in $\lambda = 1$ operation leads to high adiabatic flame temperatures, as can be seen in figure 2.2.3.

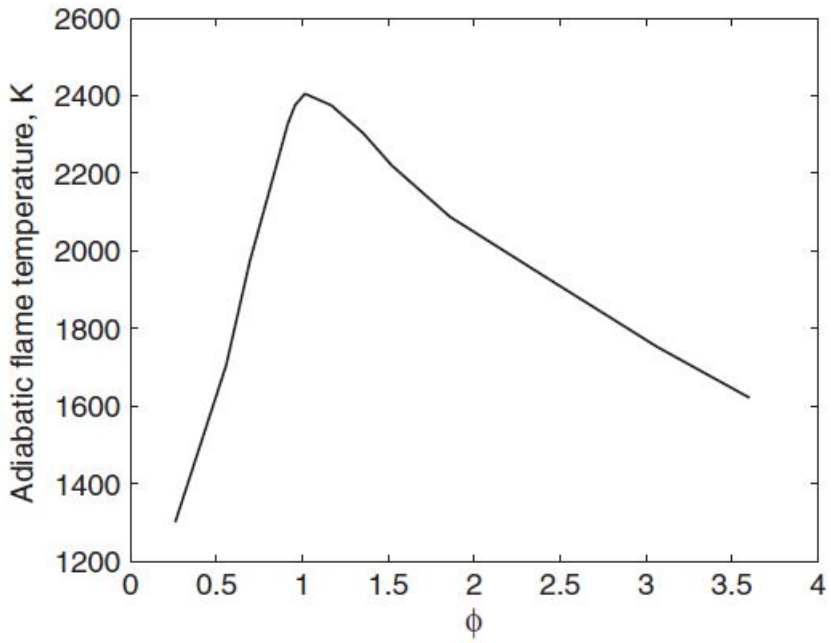

Figure 2.2.3: Adiabatic flame temperature for hydrogen-air-mixtures [54]

These high flame temperatures and the high thermal conductivity lead to extreme heating of the different combustion chamber parts. Together with the low ignition energy this leads to the mentioned pre-ignition and backfire phenomena. For this reason hydrogen fueled internal combustion engines normally operate under $\lambda > 1.5$ conditions. On the other hand, the possibility to run the engine under very lean conditions, with all its benefits, is only given because the ignition energy of very lean mixtures is still reachable with common ignitors and because the laminar burning velocity is, even under such lean conditions, high enough to guarantee a similar combustion duration as with other fuels.

Another big advantage of the lean combustion is that the only occurring emission in combustion of hydrogen, NO_X, can be avoided when $\lambda > 2$. Therefore the combustion can be almost emission free [53]. The NO_X-Emissions are pictured in figure 2.2.4 for different compression ratios as a function of the air-fuel equivalence ratio λ. Of course the induced emissions from the production of hydrogen has to be considered as well.

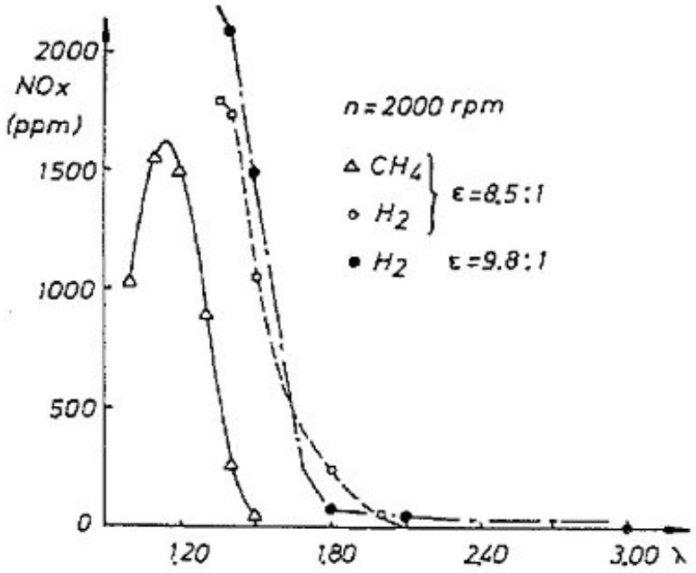

Figure 2.2.4: NO_X-Emissions as a function of the air-fuel equivalence ratio λ, for varying compression ratio ε [53]

However, the increase of λ is also reflected by a decrease of power:

$$P \sim \left(\frac{F}{A}\right) \text{ [24]}$$

The power directly depends on the fuel-air-ratio. The high flame temperature, the high thermal conductivity and small quenching gap lead to high heat losses, assuming λ=1. This drops the thermal efficiency below the level of gasoline engines. But with increasing λ the flame temperature gets lower while the laminar flame velocity still is higher than for other fuels. This results in an increase of the thermal efficiency. As shown in figure 2.2.5, the existence of gaseous fuel like hydrogen in the intake manifold is reducing the air partial pressure below the mixture pressure. This leads to a significant reduction of the volumetric efficiency. One countermeasure could be supercharging the engine with a turbo charger [24, 54].

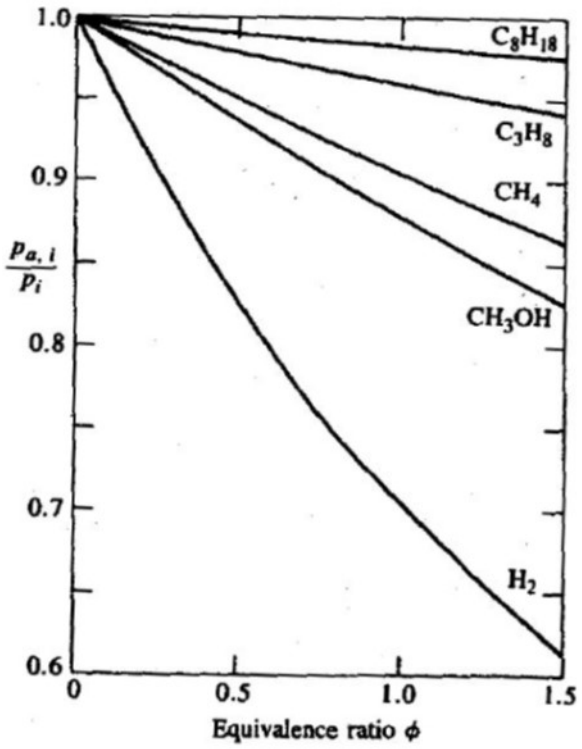

Figure 2.2.5: Effect of fuel on inlet air partial pressure [24]

The density of hydrogen is very low compared to the density of liquid fossil fuels. For that reason the storage of hydrogen is a challenge, especially in mobility applications. A tank of a conventional diesel bus can store 8,000 MJ in 200 l. To store hydrogen with a comparable quantity of energy a volume of 690,000 l at 300 K and 1 atm is necessary. Therefore the hydrogen has to be stored under high pressure or in cryogenic tanks to increase its density. The most common technology to store hydrogen are pressurized tanks with pressures ranking from 350 to 700 bar. The storage of hydrogen in metal hydrides for mobility applications is, because of their weight and charge/discharge time, not an alternative [28].

2.3 Electric Hybrid Vehicles

To reduce the fuel consumption of vehicles, hybrid powertrains are widely used in all kind of applications. Hybrids combine a conventional energy source with an alternative energy source and can be characterized by their level of hybridization. The level of hybridization ranges

between 0 for vehicles without an alternative energy source like conventional vehicles with an ICE, and 1 for vehicles that only have an alternative drivetrain like Battery Electrical Vehicles or Fuel-Cell Electric Vehicles.

Generally, hybrids can be categorized by its powertrain architecture, those with a serial power train architecture and those with a parallel power train architecture. The serial hybrid, shown in figure 2.3.1, is characterized by an internal combustion engine which gives power trough a generator to a battery system, or a fuel cell which gives electric power to a battery system. The vehicle is driven by an electrical motor which is fed by the battery system. There is no direct connection between the internal combustion engine and the drive shaft. They perform best in stop and go traffic conditions where conventional internal combustion engines are inefficient. For that reason almost all hybrid city buses are serial hybrids [18].

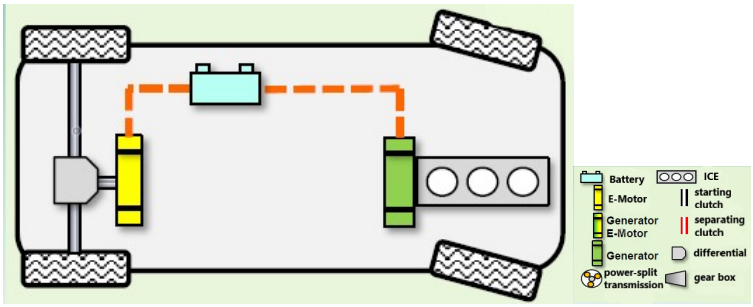

Figure 2.3.1: Serial power train architecture [18]

The parallel hybrid power train architecture is characterized by an energy source, ICE or FC, which is directly connected to the drive shaft. Apart from this mechanical power train an electrical power train is coupled to the drive shaft. The two are installed in parallel order. Figure 2.3.2 shows some possible parallel hybrid concepts [18]. As can be seen, both powertrains are not necessarily connected to each other.

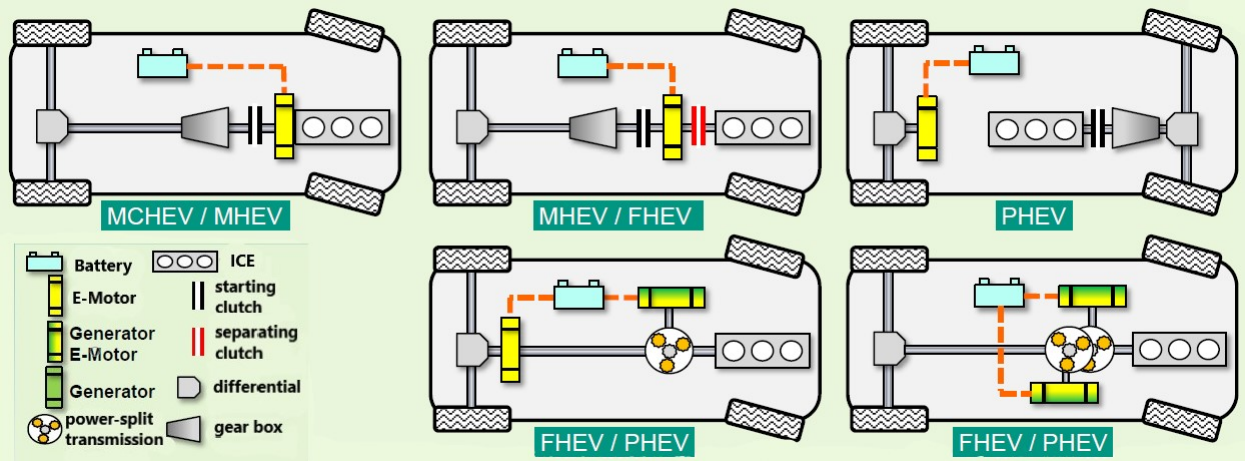

Figure 2.3.2: Parallel hybrid power train architecture, MCHEV=Micro-Hybrid, MHEV=Mild-Hybrid, FHEV=Full-Hybrid, PHEV=Plug-In-Hybrid, BEV=Battery El. Vehicle, FCEV=Fuel-Cell El. Vehicle [18]

2.4 Energy Storage System

The type, size and configuration of the electrical energy storage system is one of the most crucial decisions a manufacturer has to make in the development process because it greatly affects the performance of the hybrid vehicle. A high energy density is important to reach a high driving range whereas the power density is important for the acceleration and regeneration in which high power is needed [9, 57]. Figure 2.4.1 gives an overview over the different electrical energy storage options, picturing the power density over the energy density. Li-Ion batteries are the most common and developed batteries used for vehicle applications. This is because of its high energy density compared to other ESS. On the other hand, ultracapacitors have higher power densities, making them a very good alternative for hybrid city buses which are operating under start-stop conditions [18]. Due to the aforementioned both ESS will be used for this study. To show the differences in power density and energy density of the ESS, the most common ESS are pictured in figure 2.4.1.

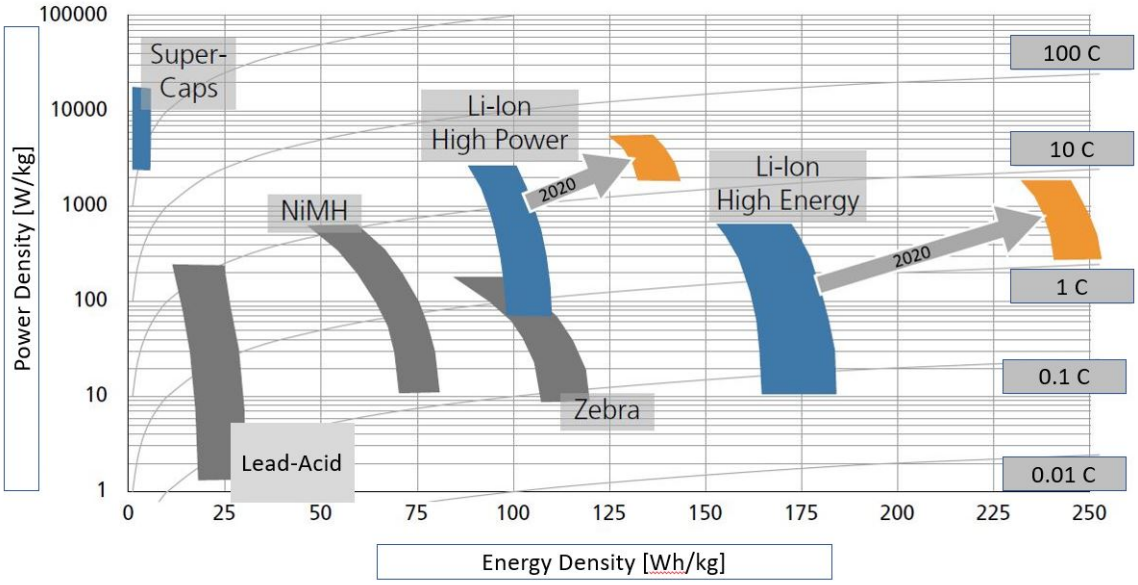

Figure 2.4.1: Different battery power densities over their energy density [18]

When it comes to vehicle applications, real operating conditions highly affect the cycling of the batteries and therefore its degeneration rate. The lifetime of the batteries is highly dependent on the depth of discharge (DOD) and the temperature. The figure 2.4.2 shows different operating strategies of Li-Ion batteries. As it can be seen, a high operating interval, keeping the State of charge between 100% and 25%, reduces the number of charge cycles dramatically. However, if the SOC can be hold between 75% and 65% a much longer lifetime can be expected [57].

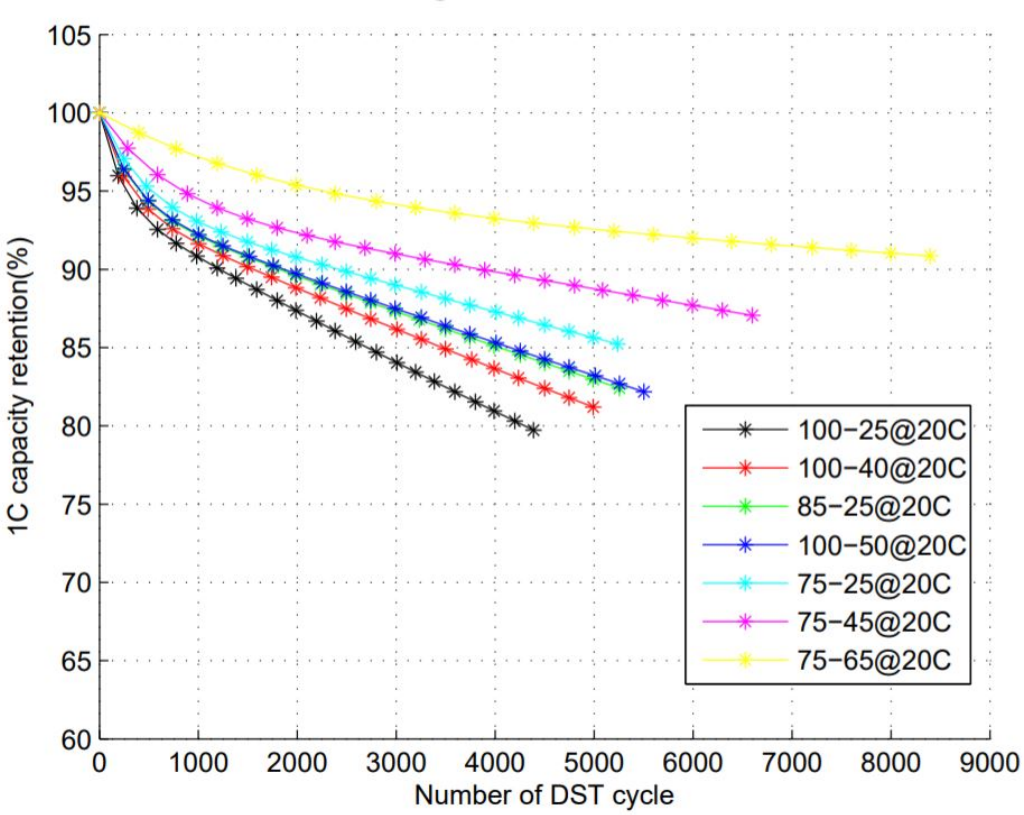

Figure 2.4.2: Capacity retention of Li-Ion batteries with different operating strategies over dynamic stress test cycles [57]

2.5 Summary

In this chapter the fundamental characteristics of hydrogen combustion are reviewed so that the foundation for the following chapters is set. The focus was put on hydrogen as a fuel for internal combustion engines. This literature review shows that hydrogen can be an alternative fuel for internal combustion engines. However, without supercharging, direct injection of hydrogen or other possible improvements the efficiency of a hydrogen fueled internal combustion engine is below the efficiency of a diesel or gasoline engine. Literature also shows that there are other benefits of running a combustion engine with hydrogen, especially under lean mixture conditions.

The literature also shows that for hybrid city buses a serial power train configuration is generally used. The stop and go traffic in big cities are conditions in which the conventional internal combustion engine is inefficient but in serial hybrids the engine can operate around its maximum efficiency, covering the mean power demand while peak power events are covered

by the electric powertrain.

To calculate the emissions and greenhouse gases it is not enough to take a look at in-service emissions only. Additionally, embodied emissions generated during the production of the vehicles and the production of the fuel have to be determined.

95% of the hydrogen is produced from fossil fuels. The main hydrogen production method is Steam-Methane-Reforming. Only 5% percent of the hydrogen comes form Electrolysis. The energy balances shows that the main part of the electricity is produced from fossil fuels and only a small part comes from renewable energy sources.

Upon this wide fundamental literature review of hydrogen fueled internal combustion engines, hybrid vehicles and energy supply a model of a hydrogen fueled internal combustion engine hybrid bus can be generated to analyze if this could be an alternative to a conventional city bus. Can a H2ICE hybrid bus show reductions in terms of consumption and GHG emissions, and how does it perform compared to a FCHB? Furthermore: Can the H2ICE hybrid bus compete with the conventional bus and the FCHB financially? All the models have to prove their performance under the urban conditions of the city of Buenos Aires.

Chapter 3

Technical Analysis of the Buses

Throughout this chapter the technical performance of the different bus platforms is evaluated under the same operating conditions. Results are than compared to those of a conventional diesel bus and amongst the different H2 platforms which include two H2ICE hybrid buses and two Fuel Cell hybrid buses. To do this first the bus operating conditions are established. After this the different bus platforms are modeled and validated. The computer simulation software Autonomie is used to create and compare the different bus models. The latter is a matlab/simulink based platform that allows modeling the different vehicle components and applying different vehicle control strategies to evaluate how a given vehicle performs under different driving conditions. To model the different vehicles Autonomie provides standard components, which were used as base units. By modifying and adjusting the matlab/simulink model of the base units and applying the vehicle control strategy, the different buses were modeled accurately.

Once the different bus models have been validated, the performance of the different platforms is established and compared.

3.1 Bus Operating Conditions

To establish the driving profile under which buses operate in the city of Buenos Aires the driving cycle developed at the Buenos Aires Institute of Technology [46] is used. The latter was developed using GPS-data from different bus lines, including streets, avenues and bus rapid transit lines, shown in figure 3.1.1 [46].

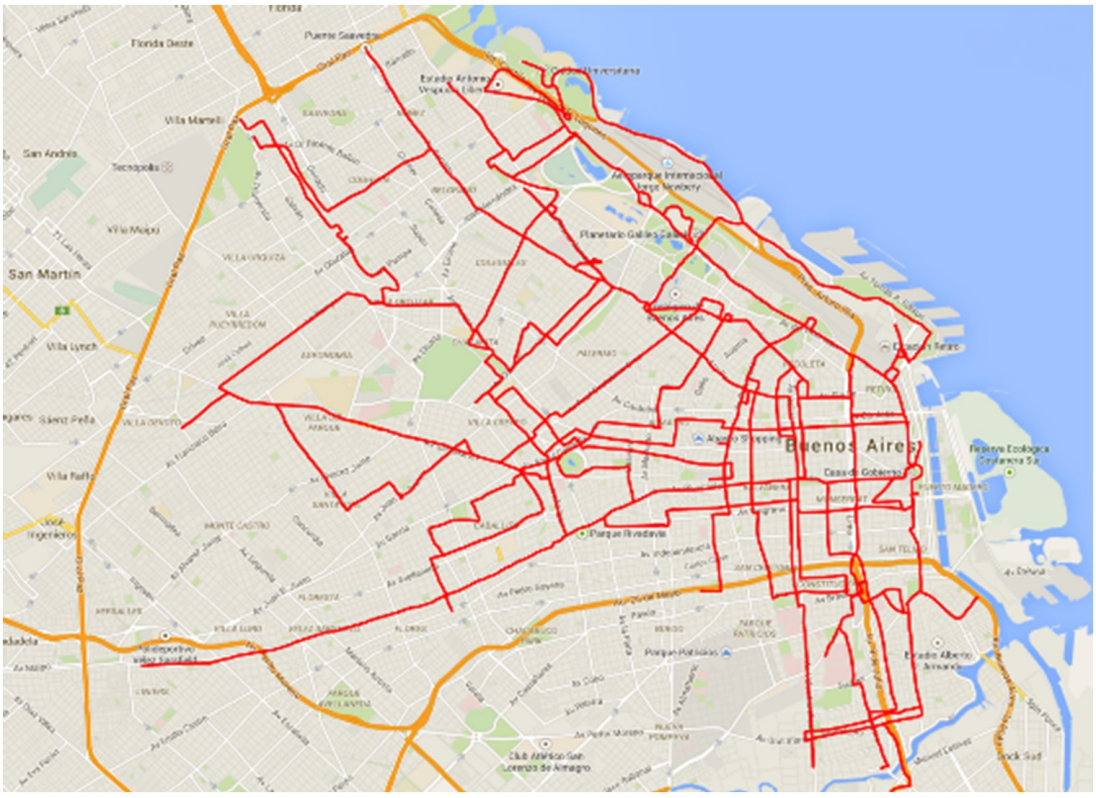

Figure 3.1.1: GPS data collected for the BADC [46]

Buenos Aires is situated on the river La Plata in a plane area without slopes. The collected GPS data were used to calculate characteristic values, like mean acceleration, mean velocity or stop time. Then, out of the characteristic values, the BADC was created, shown in figure 3.1.2. The main characteristic values can be seen in table 3.1.

Mean velocity $\frac{km}{h}$	Mean acceleration $\frac{m}{s^2}$	Cycle distance km	Time min	Idle time %
10.57	0.91	5.5	31	31

Table 3.1: Characteristic values of the BADC [46]

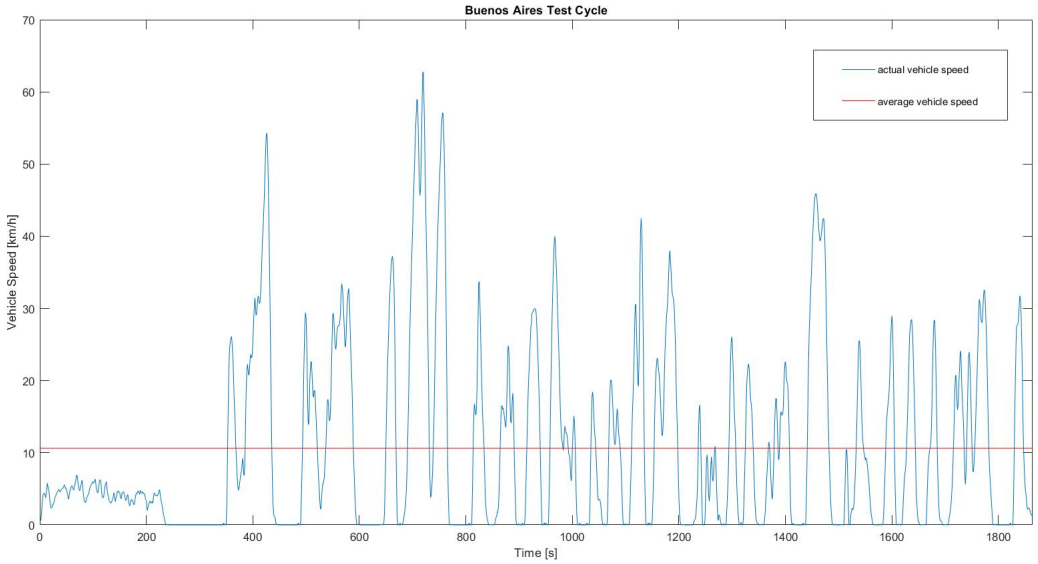

Figure 3.1.2: Buenos Aires Driving Cycle [46]

To verify that the models can accomplish the driving cycle of Buenos Aires under full load, a simulation of every model with the load of 6 tons was done. Then, to compare the different bus models the average load of 2.4 tons is assumed, which corresponds to 32 passengers of 75kg [46].

3.2 Bus Model Description, Validation

3.2.1 Conventional Bus

Model description

As reference model against which the operational, environmental and economic performance of the different hybrid vehicles can be compared, a conventional diesel bus was modeled. The reference model is based on a conventional class 8, 2-wheel drive bus, the OH 1618 L-SB from Mercedes-Benz. In Argentina and in other parts of Latin America this is a commonly used vehicle for urban public transportation. The following table 3.2 shows some technical key parameters of the bus [6, 46].

Mass	Curb [kg]	10,590
	Cargo [kg]	2,400
Body work	Frontal area [m^2]	8.06
	Drag coefficient	0.65
Wheels	Radius [m]	0.51
	Number of wheels	6
Accessories	Average power [W]	5000
Engine	Maximum power [kW]	130 @ 2200 rpm
	Maximum torque [Nm]	675 @ 1200 rpm
Gearbox	Reductions	9.2, 5.2, 3.1, 2.0, 1.4, 1
Differential	Final drive	4.3

Table 3.2: Conventional bus technical parameters [6, 46]

The conventional bus (CB) powertrain, modeled in Autonomie, is shown in figure 3.2.1.

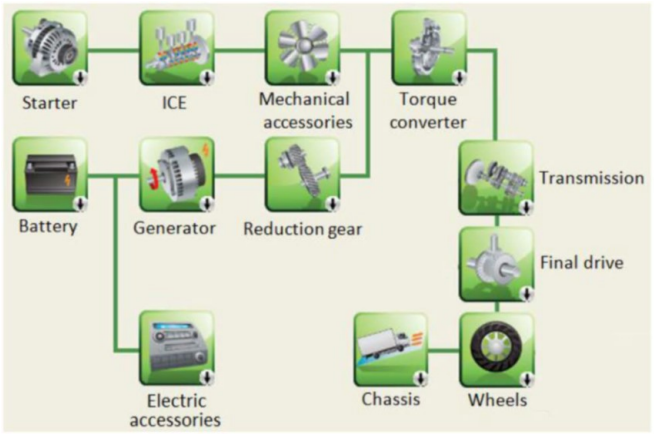

Figure 3.2.1: Power train of the conventional bus [3]

The ICE is used to drive the CB. The power flows trough the torque converter, the gearbox and a final drive to the wheels. A second power current goes through a reduction gear into a generator to produce the electricity for the electric accessories. To match the technical parameters of table 3.2, the different subsystems of the powertrain were adjusted in Autonomie.

Model validation

The validation of the CB model was done, using the Braunschweig City Driving Cycle (BCDC) and the BADC [46].

3.2.2 Fuel Cell Hybrid Bus

As zero emission reference models two Fuel Cell hybrid bus models were created. One uses Li-Ion batteries as an energy storage unit whilst the other uses ultracapacitors. The FCHB models are buses already operating in cities of Europe [10, 41]. The buses are operating in urban bus lines within the cities.

Model Description

The FCHB buses also have a series hybrid powertrain architecture but with a Fuel Cell instead of an internal combustion engine, as can be seen in figure 3.2.2.

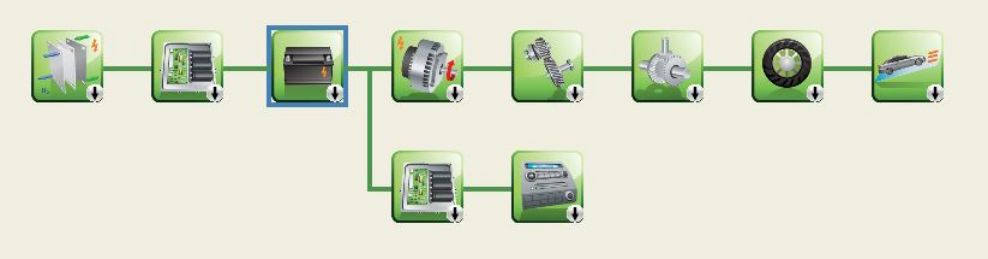

Figure 3.2.2: Fuel Cell Hybrid Bus Powertrain [3]

The following table 3.3 shows the technical key specifications of the two buses [10, 41].

	Unit	FCHV-Li	FCHV-ultra
Used in	-	Hamburg, Bolzano	London
Overall length	m	12	12
Net weight	kg	13,200	11,350
Axles	No.	2	2
Fuel Cell Power	kW	120	75
Motor Power	kW	2×120	2×67
Energy Storage Type	-	Li-Ion Battery	ultracaps
Max. Battery Power	kW	250	105
Energy Storage Capacity	kWh	26.9	2
Hydrogen Storage Capacity	kg	35	31

Table 3.3: Key specifications of the Fuel Cell Hybrid Buses [41]

Validation

To validate the models the operating conditions of the buses in London and Hamburg were replicated and results compared to those obtained by the buses in the field. Key parameters for the bus lines are the average velocity, the stops per kilometer and the length of the line [10]. Knowing the key parameters of the bus lines in London and Hamburg, driving cycles with similar conditions were used to replicate the operation. Then the consumption of the bus models in these driving cycles was compared with that of the buses operating in the different cities.

Operating conditions in London were replicated using a Washington Driving cycle (WMATA), shown in figure 3.2.3. It is a cycle created based on real driving data from Washington D.C. The characteristics of the cycle are similar to the driving conditions of the bus line in London [23, 44]. Table 3.4 shows the key parameters of the bus lines and the driving cycles.

	Distance	Av. speed	Stops per km
Bus line London	6.2	12.4	3
WMATA	7.3	13.7	3.2
Bus line Hamburg	9.6	19.3	2.6
BCDC	10.9	22.6	2.7

Table 3.4: Key parameters of the bus lines and the driving cycles [23, 41]

For the bus line in Hamburg the BCDC, already mentioned in 3.2.1 and shown in figure 3.2.4, was used. An overview of the parameters and the hydrogen consumption of the bus lines and the driving cycles are summarized in table 3.5.

It is important to remark that the driving cycles do not exactly reproduce the bus operation within the lines of Hamburg and London and that there are minimal discrepancies like a minimal higher average velocity. However they are coming close and can be used to validate the models.

	Simulation	Bus line	Discrepancy
FCHB-Li [kg/100km]	8.1	8	<2%
FCHB-ultracaps [kg/100km]	9.9	9.7	2%

Table 3.5: Fuel consumption of the FCHB models over the BCDC and the WMATA

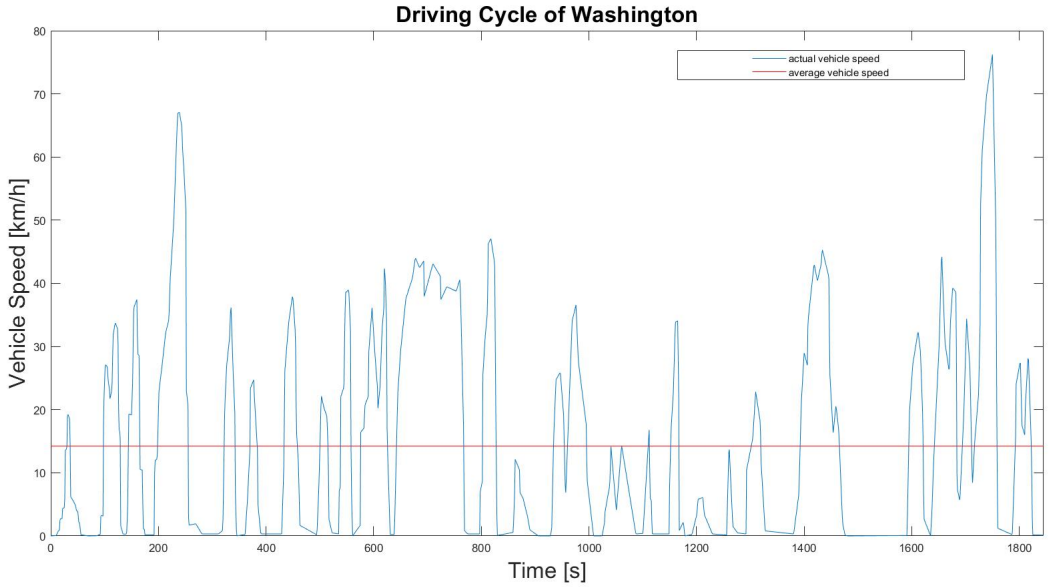

Figure 3.2.3: WMATA-Cycle

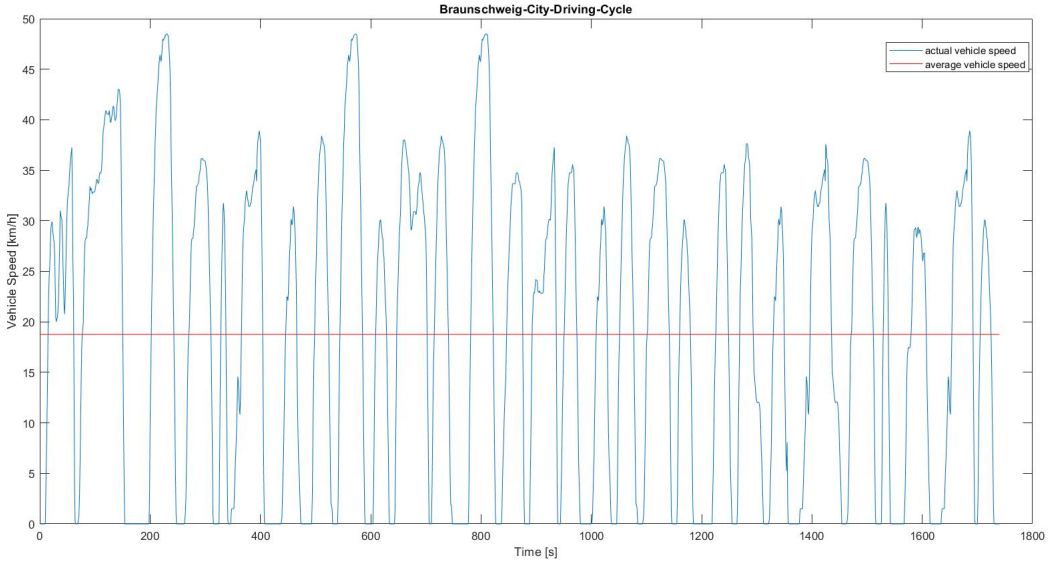

Figure 3.2.4: Braunschweig City Driving Cycle (BCDC)

With a similar average velocity and a similar number of stops per kilometer it can be said that the lines and the driving cycles are comparable [41, 44]. The higher consumption of the simulations can be explained because of the minimal higher average velocity. However, the discrepancy is below 2% which validates the computational bus models.

3.2.3 H2ICE Hybrid Bus

Model Description and Validation

On the basis of a developed and validated series hybrid electric bus platform [46], two H2ICE hybrid bus models were created. The used basis platform was also developed for driving conditions in Buenos Aires. Therefore, the electric consumption of additional electric devices and mechanical losses are adopted from the series hybrid electric bus platform. As the Fuel Cell hybrid buses, one of the two H2ICE hybrid buses has a Lithium-Ion battery pack (H2ICE-Li) as an energy storage unit, whilst the other uses ultra-capacitors (H2ICE-ultracaps). The power train configuration can be seen in figure 3.2.5.

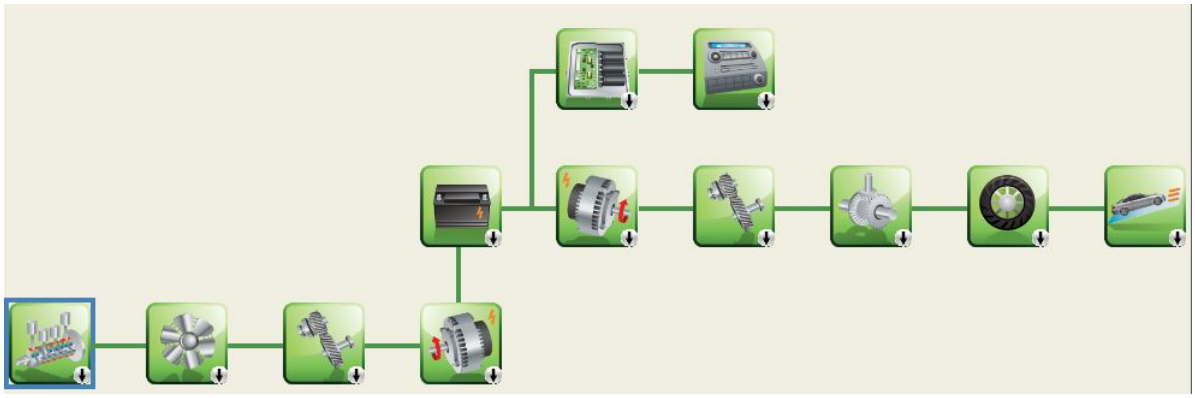

Figure 3.2.5: H2ICE hybrid bus powertrain [3]

Because the engine is separated from the drive shaft, the H2ICE can perform at its optimum efficiency condition to charge the battery avoiding the efficiencies incurred by engines when operating in a highly transient mode like those related to public buses traffic conditions.

As the CB is the reference platform, the chassis parameters like the frontal area, drag coefficient and length of the bus are adopted from the CB model. Additionally an energy recuperation system is added as well as the hydrogen storage system.

With the aim of coming close to the range of conventional city buses, 35kg of hydrogen are needed. As described in 2.2.2, with high pressure gaseous hydrogen storage tanks and cryogenic tanks, two potential possibilities are available for mobile applications. However, high pressure gaseous hydrogen tanks have a much better volume-cost ratio than cryogenic tanks and are therefore the most used type of hydrogen storage in mobile applications [2, 16, 25, 50, 51, 58]. To achieve the 35 kg of hydrogen, tanks with a storage volume of 40 liters at 70 MPa and total weight of approximately 900 kg are installed.

For the H2ICE, the initialization parameters of the combustion fuel were modified from

diesel characteristics to hydrogen characteristics. Some important fuel parameters are shown in table 3.6.

	diesel engine	hydrogen engine
Fuel Density [kg/l]	0.835	0.0899×10^{-3}
Fuel Heating Value [kJ/kg]	42,5000	120,000
Fuel Carbon Ratio [kg/kg]	$\frac{12}{13.8}$	0
Engine Power [kW]	130	80

Table 3.6: Changed parameters of the H2ICE

The fuel density, the heating value and the carbon ratio are important characteristics of the engine fuel as already described in chapter 2. To achieve the benefits of a lean operation, like the avoidance of NO_X-Emissions [52, 54], a $\lambda \approx 2.5$ operation point is chosen. However, this lean operation point leads to an engine power reduction [47]. Therefore the maximum engine power, the torque curves and the fuel map of the H2ICE were accordingly scaled down, whereas the efficiency of the engine maintained the same, shown in figure 3.2.6.

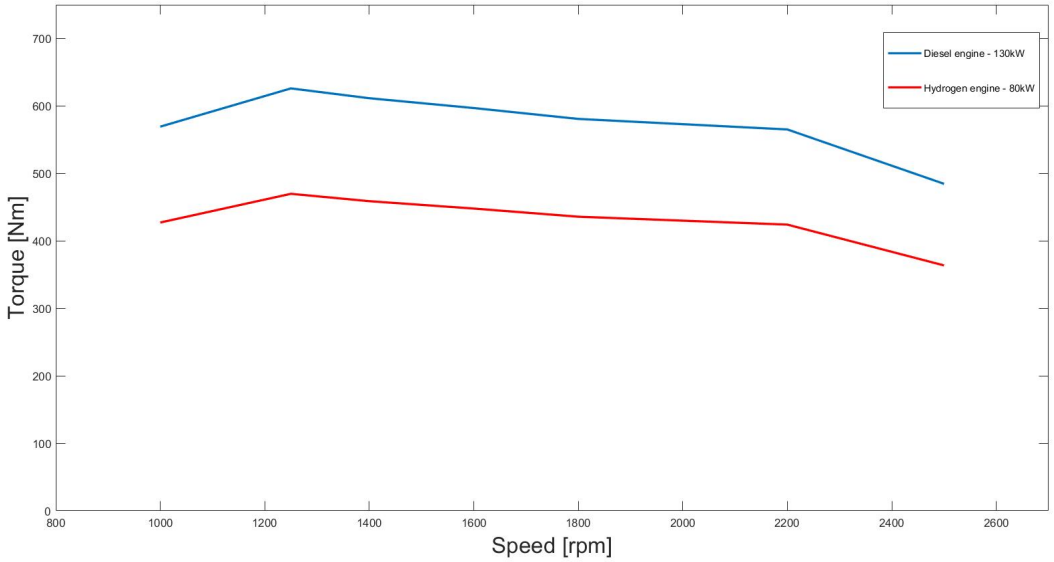

Figure 3.2.6: Torque curves of diesel engine and down scaled hydrogen engine

The down scaled fuel map from the diesel engine was modified to a hydrogen fuel map, using the following formula:

$$P = \dot{m}_{diesel} \times H_{u_{diesel}}$$

Out of the Energy amount the necessary amount of hydrogen was calculated with:

$$\dot{m}_{hydrogeno} = \frac{P}{H_{u_{hydrogen}}}$$

Optimum Bus Configurations

The hardest conditions for an internal combustion engine are the starting conditions. For that reasons the limits of the state of charge (SOC) of the electrical storage system were optimized so that the H2ICE does not have to start and stop in short intervals. The SOC describes the actual charging state of the batteries and is highly responsible for the lifetime of the battery. If the battery is deeply cycled the lifetime of the batteries is reduced dramatically [18, 57].

Figure 3.2.7 shows the lifetime of different electrical storage systems with the charge/discharge frequency of the BADC. For the Li-Ion batteries a storage capacity of 42kWh is necessary so that the battery pack hold up the 10 years lifetime of the bus, whereas in case of ultra capacitors only a storage capacity of 3 kWh is necessary [46].

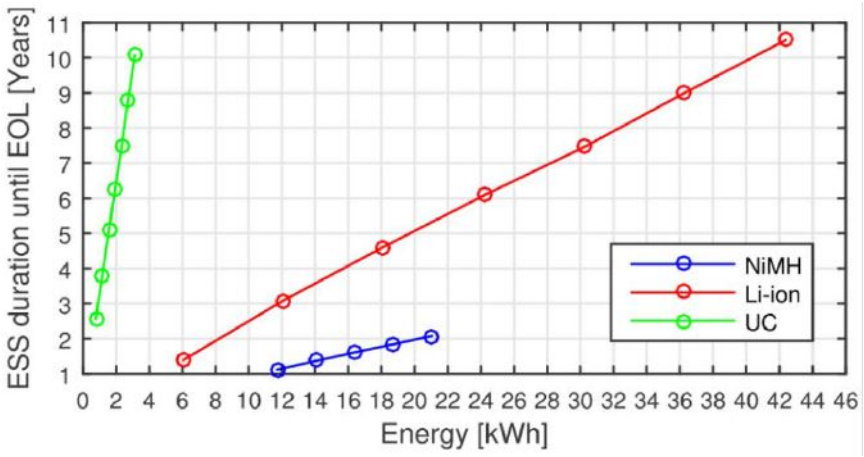

Figure 3.2.7: Life Time of different electrical storage systems [46]

To determine the lowest fuel consumption different motor/generator ratios were tested. As can be seen in figure 3.2.8 and 3.2.9, which are showing the fuel consumption of the buses with different motor/generator ratios and different ESS, the bus models reach the lowest fuel consumption with the motor generator ratio of 100kW/80kW. To avoid an ESS replacement and to reach the lowest fuel consumption, the Li-Ion model was created with an ESS capacity of 42kWh and the ultracapacitor model with an ESS capacity of 3kWh.

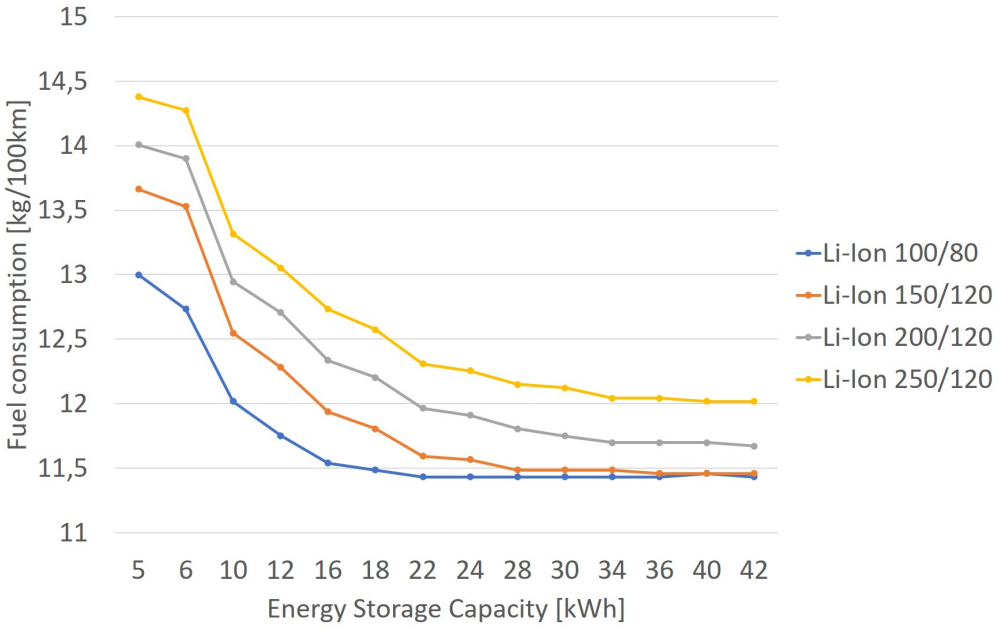

Figure 3.2.8: Fuel consumption of different motor/generator ratios as a function of ESS (Li-Ion) capacity

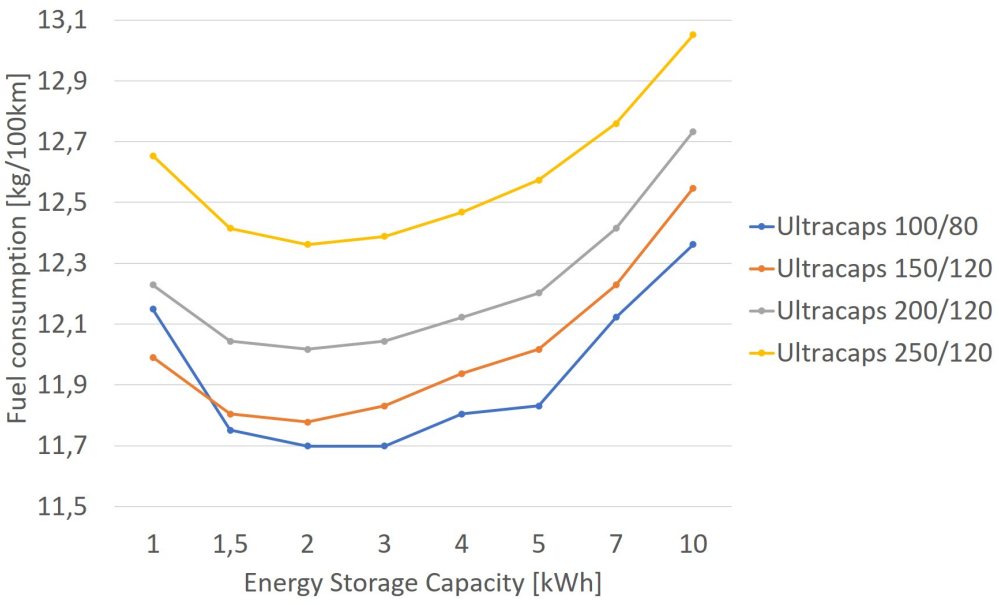

Figure 3.2.9: Fuel consumption of different motor/generator ratios as a function of ESS (ultracapacitors) capacity

Looking at the fuel consumption of the model with ultracapacitors, it can be seen that the

consumption increases after reaching a minimum. This can be explained by the high specific weight of ultracapacitors.

3.3 Fuel consumption

Table 3.7 shows the consumption of the different bus models on the BADC. The consumption is shown per 100km and for the lifetime of the buses. For the lifetime consumption a lifetime of 10 years and 75,000 km per year is assumed what is an accurate assumption for buses operating in Buenos Aires [15, 46].

BADC	H2ICE-Li	H2ICE-ultracaps	FCHB-Li	FCHB-ultracaps
H_2 $[\frac{kg}{100km}]$	11.5	11.7	10.3	10.9
$H_2[\frac{kg}{Lifetime}]$	86,054	87,062	77,590	81,419

Table 3.7: Consumption of the Buses with a load of 2.4 tons

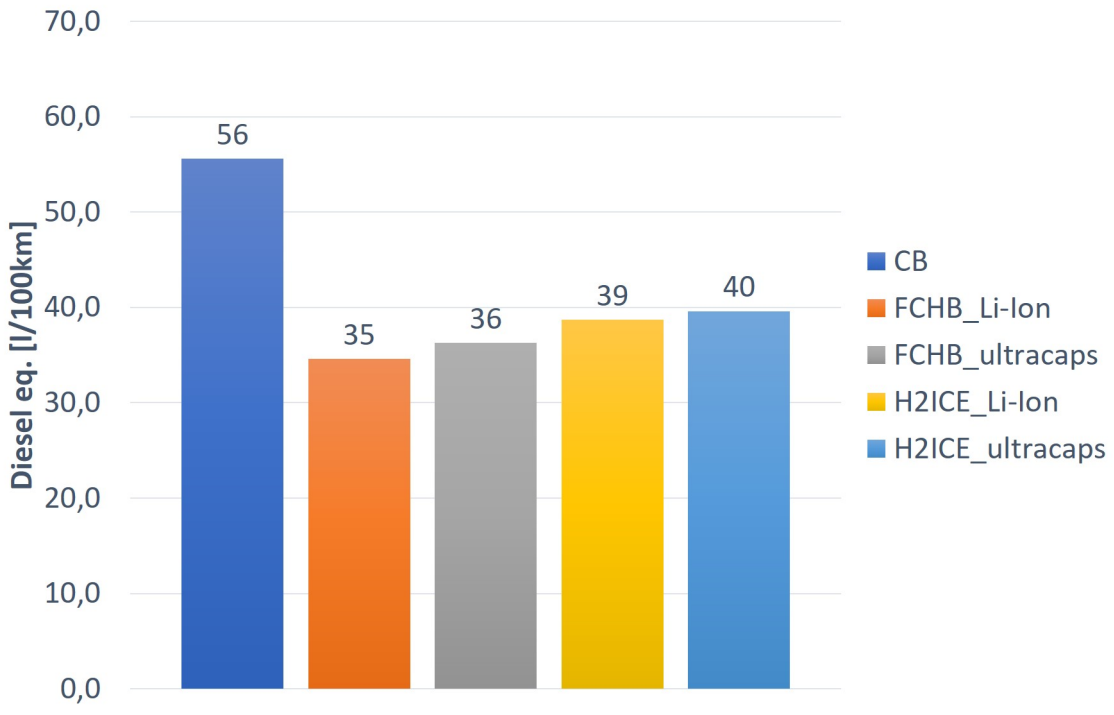

Figure 3.3.1: Fuel Consumption in Diesel eq. per 100km

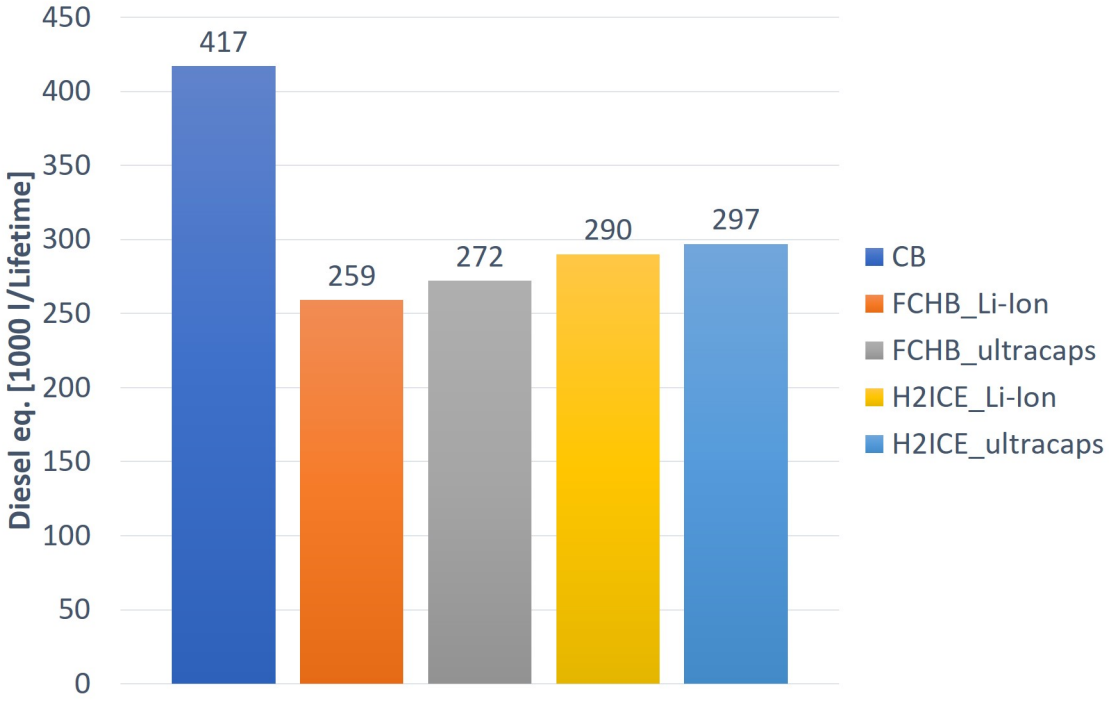

Figure 3.3.2: Fuel Consumption in Diesel eq. per lifetime

As can be seen in figure 3.3.1 and figure 3.3.2 the hybrid buses can document big benefits in consumption: The H2ICE hybrid bus model with Li-Ion batteries has 31% less consumption than the conventional diesel bus model but a 11% higher consumption than the Fuel-Cell hybrid bus with Li-Ion batteries. The H2ICE model with ultracapacitors reduces the consumption by 29% compared to the CB model but has a 10% higher fuel consumption than the Fuel Cell hybrid bus model with ultracapacitors. The comparison between the bus models, with same hydrogen engine but different ESS, has shown, that the models using ultracapacitors have a 3% higher consumption than the ones with Li-Ion batteries. That applies for both hydrogen fueled models: the H2ICE model and the Fuel Cell model.

3.4 Conclusions

A consumption reduction of over 30%, compared to the conventional buses, can be reached by the H2ICE bus models. This shows that hydrogen fueled hybrid buses have a high potential to save fuel. The fuel reduction mainly comes from the hybrid power train architecture. However, the H2ICE hybrid bus models can not outperform the Fuel-Cell Buses, which have, owing to their higher efficiency, an even lower fuel consumption. Because of their lower weight, the

models with Li-batteries have a minimal lower fuel consumption than the models with ultra-capacitors. Now that all the buses are accordingly modeled and validated and a consumption simulation was done a closer look can be taken on the environmental impacts.

Chapter 4

Life Cycle Emission Analysis

Based on the fuel consumption results attained in the previous chapter for each bus it is now possible to asses the life cycle emissions of the different vehicles. To do this the Greenhouse Gases, Regulated Emissions, and Energy use in Transportation (GREET) Model by Argonne National Laboratory is used. The calculation is divided in two parts, the in-service emissions and the embedded emissions. The global warming potential of the different gases is established based on the 100-year time horizon. Table 4.1, shows the GWP of the different gases [27].

GHG	Global Warming Potential
CO_2	1
CH_4	28
N_2O	265

Table 4.1: AR5/GWP [27]

4.1 Fuel Based in-Service Emissions

Fuel based emissions are calculated from well to wheel (WTW) as to include both direct and indirect fuel emission [19, 55].

- Direct Emissions: Emissions produced by the vehicle during operation.
- Indirect Emissions: All emissions produced during the production of the fuel including the production of the primary energy source, the transport to the refineries and the production of the fuel.

4.1.1 Conventional Bus

Both the direct and indirect fuel based emissions of a conventional diesel bus, are shown in table 4.2. Indirect emissions depend on many factors, the origin of the oil, the efficiency of the refining process, etc [36]. Since direct emissions are produced by vehicles during operation, they depend highly on the fuel consumption of the vehicle.

Table 4.2 gives an overview over the emissions produced by the conventional bus model. Beneath the GHG emissions diesel fueled vehicles produce a series of other emissions which have impact on the air quality in cities but are not included in the emission analysis.

	Unit	Indirect Emissions	Direct Emissions	Total Emissions
CO_2	$\frac{g}{km}$	250	1498	1748
CH_4	$\frac{g}{km}$	2	12×10^{-3}	2
N_2O	$\frac{g}{km}$	4×10^{-3}	46×10^{-3}	50×10^{-3}
CO	$\frac{g}{km}$	0.4	1.6	2
NO_X	$\frac{g}{km}$	0.6	0.6	1.2
PM_{10}	$\frac{g}{km}$	0.006	0.14	0.15
$PM_{2.5}$	$\frac{g}{km}$	0.04	0.08	0.12
SO_X	$\frac{g}{km}$	0.4	0.02	0.42

Table 4.2: Diesel Well-to-Wheel Emissions [36]

4.1.2 Hydrogen fueled Buses

Although hydrogen fueled vehicles can have zero tank to wheel (TTW) emissions, the indirect emissions associated to the hydrogen production can vary significantly. As shown in figure 4.1.1, 94% of the hydrogen is produced from fossil fuels and only 4% from electrolysis. In Argentina almost all hydrogen produced comes from the reforming of natural gas [45]. To asses the potential impact of the hydrogen stream on the vehicle's GHG emissions four different scenarios are taken in account.

The first scenario assumes production of hydrogen by SMR, whilst the second and third assume electrolysis based production from two different power generation sources. The second scenario assumes composition of power generation sources from the actual energy balance of Argentina [12] whilst the third scenario assumes the expected composition of power generation in 2025 [13]. The fourth scenario assumes electrolysis based production from renewable power generation sources.

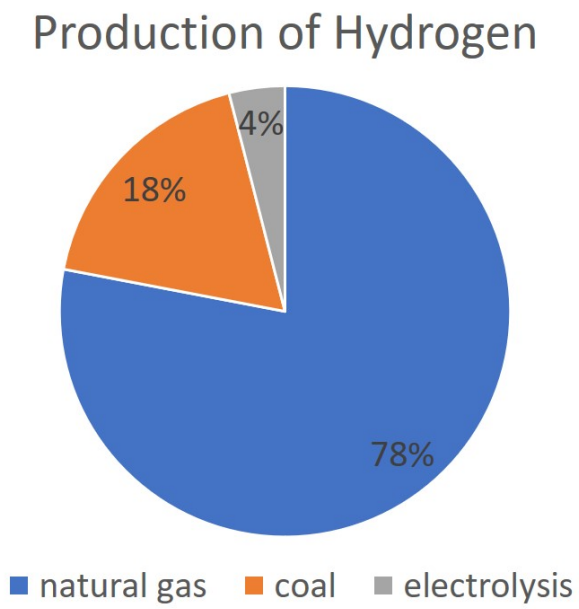

Figure 4.1.1: Production of Hydrogen by sources[32]

The first scenario assumes that H2 is produced via SMR. Figure 4.1.2 shows the different efficiencies assumed for the entire Well to Tank (WTT) process [36]. Also, losses in the recovery of natural gas and in the compression of hydrogen were taken in account [36]. The following figure 4.2.1 shows the production process of hydrogen from natural gas with the efficiencies and greenhouse gas emissions for each stage of the production process. After extracting the subterranean natural gas with an efficiency of 97% and 4.8g produced CO_{2eq} per MJ extracted gas, pipelines transport the natural gas to the SMR refineries. During transportation rarely any losses occur and a transportation efficiency of 100% can be assumed. Once reached the refineries, the natural gas is used to produce hydrogen through SMR as explained in chapter 2. While doing so, the reformer, working with an efficiency of 72%, emit 81g CO_{2eq} per MJ produced hydrogen. After a lossless transfer to hydrogen fuel stations the hydrogen is compressed with an efficiency of 91.5%. During the hydrogen transportation and compression process 18.5g CO_{2eq} per MJ compressed hydrogen are emitted.

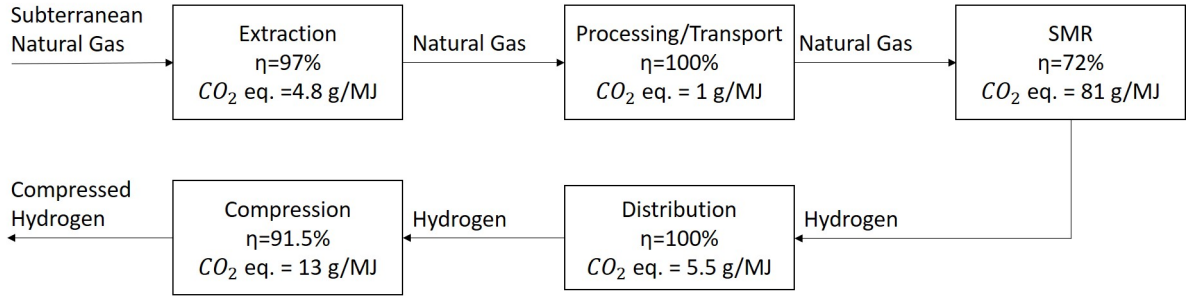

Figure 4.1.2: Production process of hydrogen from natural gas [36]

As mentioned above scenarios 2 and 3 assume that H_2 is produced from electrolysis. As expected the electricity generation source has a big impact on the well-to-wheel emissions. Figure 4.1.3 shows the electricity generation profile of the Argentine grid [12] whilst figure 4.1.4 shows the expected electricity generation profile of the Argentinian grid in 2025 [13].

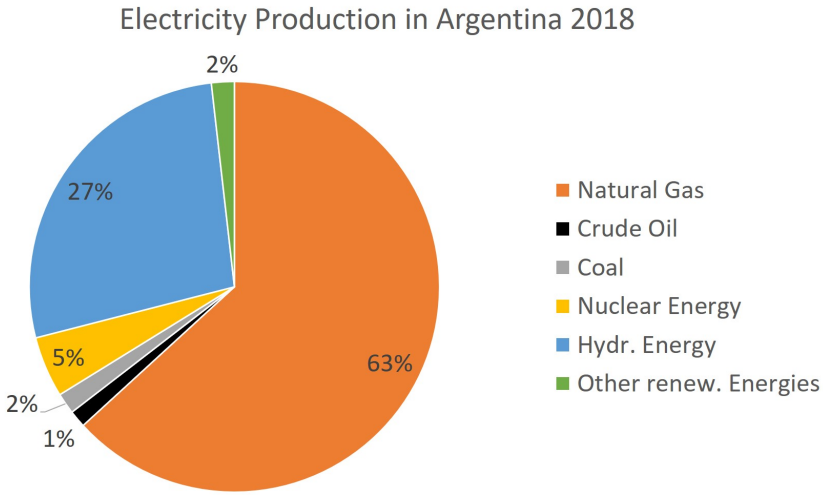

Figure 4.1.3: Actual electric grid composition in Argentina [12]

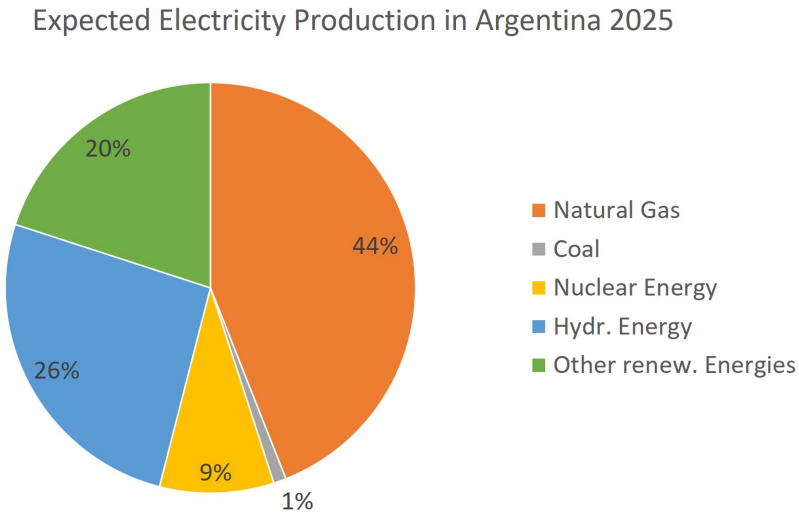

Figure 4.1.4: Expected electric grid composition in Argentina in 2025 [13]

Figure 4.1.5, shows the well to tank emissions of hydrogen production if the later is powered by electricity with the average carbon foot print of the today's Argentine grid.

- In the case of oil based thermal generation an overall power plant efficiency of 46% is assumed. Losses in the extraction of the petroleum and in the refinery were taken in account [36].
- For natural gas a power plant efficiency of 57% was assumed and losses in the extraction are included [36].
- For coal a power plant efficiency of 41% was assumed and the losses in mining are included [22].

As shown above, nuclear and renewable energy account for 34% of the average electricity generation. The latter is assumed to be 0 emission power. Finally the electrolyzer efficiency is assumed to be 71.5% [36]. The whole production process can be seen in figure 4.1.5.

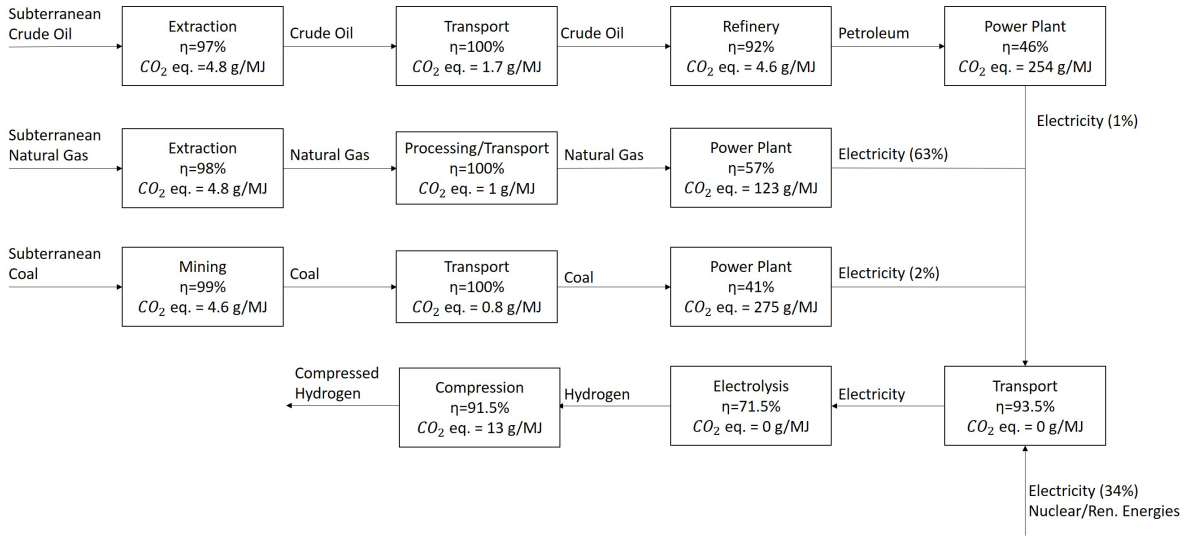

Figure 4.1.5: Production process of hydrogen from electricity using the grid of Argentina [36]

Reducing the amount of thermal power generation sources to 45% and increasing renewable power generation sources to 46%, as it is expected for 2025, leads to the third scenario.

As fourth scenario electrolysis based hydrogen production with renewable energy sources is taken in account. One option could be surplus electricity produced by renewable energies which can not fed into the grid because of variations in the grid, occurring when the renewable energy part of the grid composition is too high.

Table 4.3 lists the indirect, direct and total greenhouse gas emissions for the three scenarios, showing that the production of hydrogen using a SMR has a lower carbon foot print that when using electrolysis powered with electricity from today's grid of Argentina. However, the analysis also shows that the carbon foot print using electrolysis based on an electricity grid with an higher percentage of renewable energies can be reduced significantly. As can be seen in scenario three, using 46% renewable energy sources in electricity production the carbon foot print of the electrolysis is almost the same as using natural gas in the production of hydrogen. Increasing the part of renewable energy in the production of electricity the carbon foot print of the hydrogen production process decreases even more until being a zero GHG emission production process as in scenario four.

	Unit	Indirect Emissions	Direct Emissions	Total Emissions
Hydrogen from Natural Gas	$\frac{g}{MJ}$	116	0	116
Hydrogen form Electrolysis (Actual Grid Argentina)	$\frac{g}{MJ}$	165	0	165
Hydrogen from Electrolysis (Grid Argentina 2025)	$\frac{g}{MJ}$	115	0	115
Hydrogen from Electrolysis (Renewable Energy Sources)	$\frac{g}{MJ}$	0	0	0

Table 4.3: GHG Emissions in the four scenarios [22, 36]

Based on the GHG emission intensity of the different hydrogen production pathways it is possible to establish the energy specific well to tank CO_2 emissions of the different proposed H_2 production scenarios. Results are shown in Table 4.3.

4.1.3 In-Service Greenhouse Gases

With the lower heating value of the fuels, the carbon intensities described above and the fuel consumption of the different vehicles it is possible to establish the well to wheel carbon foot print of different evaluated buses under the Buenos Aires driving conditions. Figures 4.1.6 and 4.1.7 show the fuel based in-service GHG emissions attained by the different vehicles under the established operating condition.

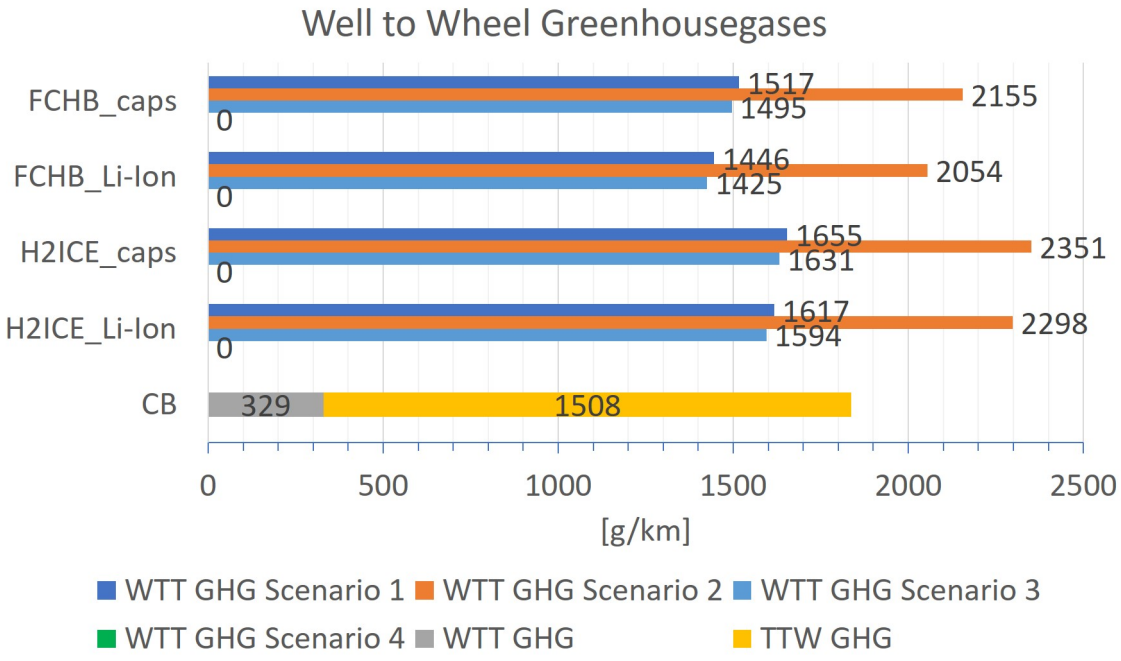

Figure 4.1.6: Well-to-Wheel CO_2 eq. of the different bus models

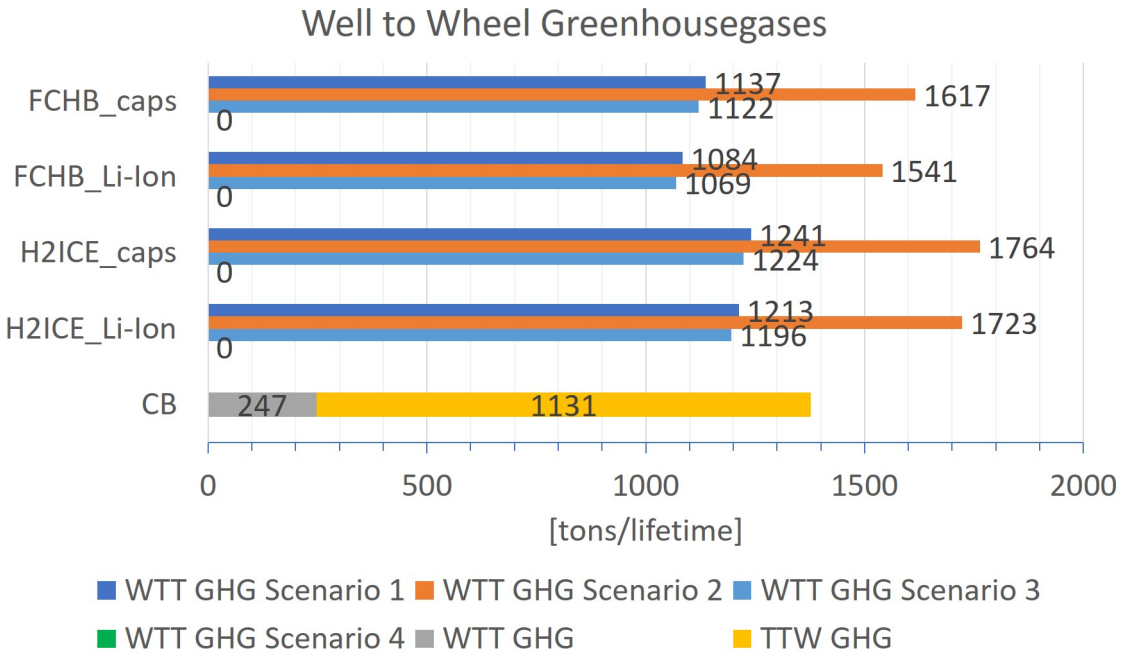

Figure 4.1.7: Well-to-Wheel CO_2 eq. of the different bus models

As can be seen, using a SMR in the production of hydrogen, the H2ICE hybrid bus models

can reduce the GHG emissions about 12% whilst the Fuel Cell hybrid bus models reduce the GHG emissions about 17%. Using electrolysis in the production of hydrogen the analysis has shown that only with an increase of renewable power generation sources GHG emissions can be reduced. With today's composition of power generation sources a reduction of GHG emissions can not be realized and even with the much lower fuel consumption all hydrogen fueled bus models show significant higher GHG emissions. However, assuming the 2025's expected composition of power generation sources for electrolysis process the hydrogen fueled bus models reach the same, or even a minimal higher, emission benefit that when using SMR in hydrogen production process. Furthermore, the 4 scenarios show that incrasing the amount of renewable energy the efficiency benefit of the fuel cell hybrid buses over the H2ICE hybrid buses become more and more irrelevant. Looking at the GHG emissions in figure 4.1.6 and 4.1.7, scenario four shows that with electricity based on 100% renewable energy sources the fuel cell buses do not have any benefits over the H2ICE hybrid buses, even they have a 10% higher efficiency.

4.2 Embedded emissions

The embedded emissions includes all emissions emitted during production, lifetime and recycling of a product. To establish the embedded emissions of the different vehicles a Life Cycle Inventory (LCI) of these is undertaken. The inventory takes into account emissions generated by the production of materials, vehicle manufacture and assembly (VMA) and the disposal/recycling end of life (EOL) process. As for the calculation of fuel use indirect emissions, GREET is used to calculate the embedded emissions of the different vehicle platforms. Based on the weight of the different vehicle components, the computational tool estimates the type and quantity of materials used for the manufacturing of the latter and subsequently calculates the embedded emissions (EEE) of vehicle production process. These are divided into four categories: Vehicle material, batteries, fluids and assembly disposal and recycling (ADR)[38, 39].

4.2.1 Bus embedded Greenhouse Gases

GREET has three basic platforms: Passenger Cars, Sport Utility Vehicles and Pick-Up Trucks. Therefore, one of these platforms had to be adapted to that of a bus. Using the pick-up platform as starting point and modifying the components weight to match those of the modeled bus platforms GREET can calculate the embedded emissions of the evaluated bus models.

Conventional Bus

The weight of the different bus parts was taken from the vehicles specification spreadsheet provided by the manufacturer. These are shown in table 4.4.

	Components weight [%]	EEE [t]
Powertrain System	11%	3.6
Transmission System	3%	1.3
Chassis/Body	86%	29
Total weight [kg]	10,590kg	34t

Table 4.4: Components weight and EEE for the CB [3, 37]

Fuel Cell Hybrid Bus

The FCHB model is based on a FC PUT. The weight of the components relative to the H2 fuel line, storage and fuel cell were taken from datasheets [41] and can be seen in table 4.5.

	FCHB-Li		FCHB-ultracap	
	Weight [%]	EEE [t]	Weight [%]	EEE [t]
Powertrain System	0.8%	2.3	0.9%	2.3
Transmission System	3%	1.8	3.2%	1.8
Chassis/Body/H_2-Tank	83.6%	41	83.4%	36
Fuel Cell System	8.6%	15.3	9%	14.4
Motor	1.3%	0.5	1%	0.3
Electronic Controller	0.3%	0.1	0.4%	0.1
Batteries	2.4%	1.8	3%	2.3
Total	13,200t	63	11,350t	57

Table 4.5: Component weights and EEE for the FCHB models [3, 37]

H2ICE Hybrid Bus

To estimate the EEE of the H2ICE hybrid the PUT hybrid electric vehicle platform was modified to match the H2ICE composition. These was done for both the Li-ion battery and the ultracapacitor platforms. Since GREET does not include an ultra capacitor ESS, the materials of the battery ESS were changed to match those of an ultra capacitor [4, 30]. The weight of the components is shown in table 4.6.

	H2ICE-Li		H2ICE-ultracap	
	Weight [%]	EEE [t]	Weight [%]	EEE [t]
Powertrain System	10%	4.4	10%	4.4
Transmission System	2.5%	1.7	2.4%	1.7
Chassis/Body/H_2-Tank	82%	31.5	82%	31.5
Motor	1%	0.17	0.9%	0.17
Generator	0.5%	0.25	0.4%	0.25
Electronic Controller	0.4%	0.1	0.3%	0.1
Batteries	4%	2.4	4.4%	2.9
Total	12,000 kg	40.5t	12,500t	41t

Table 4.6: Components weight and EEE for the H2ICE hybrid buses[3, 37]

4.2.2 Embedded Greenhouse Gases

Using the weights of the different vehicle components, the computational tool estimates GHG emissions produced during the production process of the different components. The results are shown in figure 4.2.1.

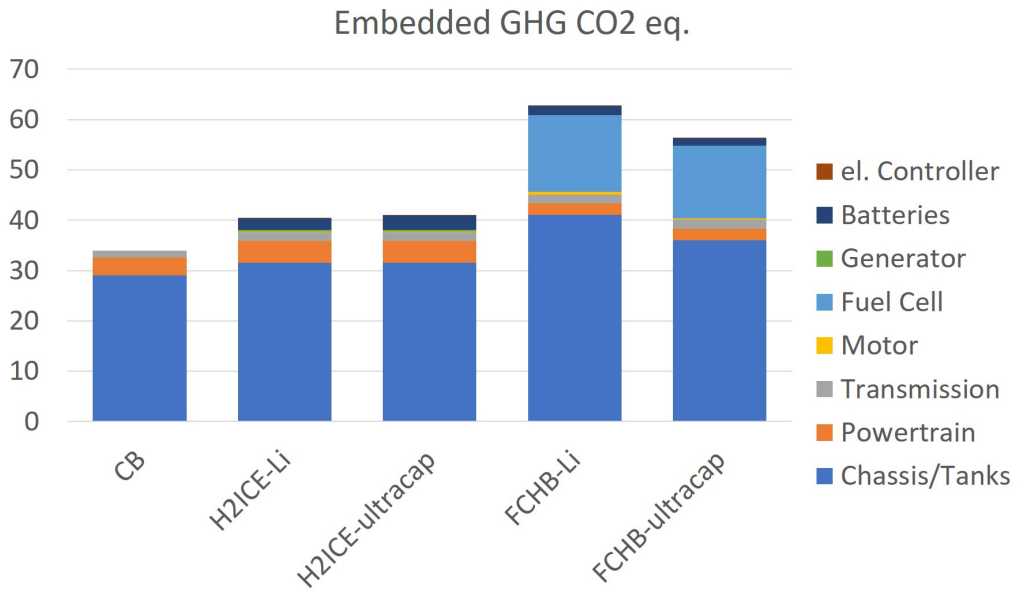

Figure 4.2.1: Embedded GHG's of the different Buses [37]

Compared to the CB all hydrogen fueled hybrid bus models show higher EEE. The H2ICE models have minimal higher EEE due to their additional batteries and H_2-storage tanks, whereas

the FCHB models show significant higher EEE due to the additional high-emission fuel cells.

4.3 Life-Cycle Emissions

Now that the In-Service emissions and the EEE have been calculated the overall life cycle emissions of the bus platforms can be estimated. Overall results are shown in figure 4.3.1.

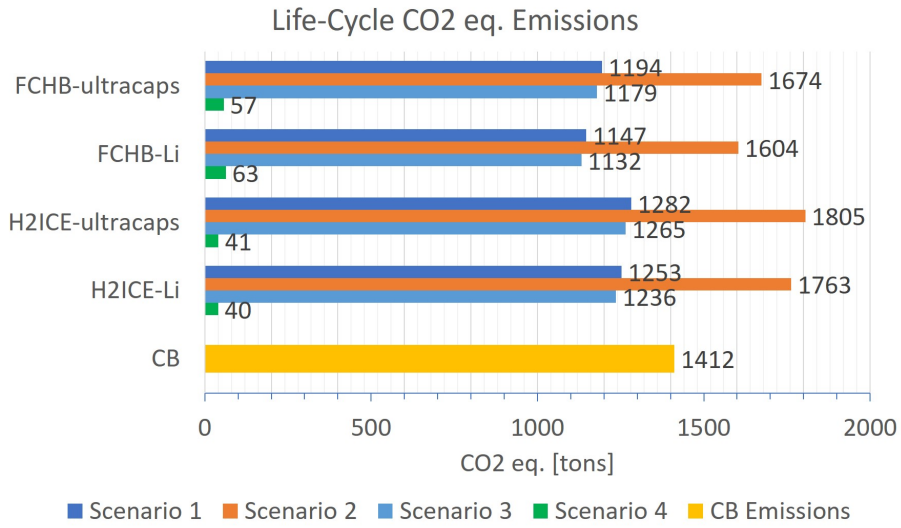

Figure 4.3.1: Life cycle GHG's with hydrogen from natural gas

As shown in Figure 4.3.1 scenario 1, were hydrogen is produced by SMR all hydrogen fueled buses show lower GHG emissions than the CB. About 95% of the emissions are related to in-service emissions, showing that in the case of buses, EEE are negligible compared to fuel based emissions. Lower fuel consumption of the fuel cell hybrid buses results in the lower life cycle GHG emissions. This is mainly due to the high efficiency of the power unit.

In scenario 2, where H2 is produced using electricity with the average carbon foot print of the Argentine grid, the GHG's of the hydrogen fueled buses are higher than those of the CB. The lower fuel consumption of the hybrid buses does not offset the high GHG emissions of the electric grid.

On the other hand, the result shows that if hydrogen is produced using electricity with the average carbon foot print of the 2025's expected Argentine grid, the GHG emissions are lower than those of the CB and even lower than the GHG emissions in scenario 1.

Assuming electricity based on renewable energies like in scenario 4, the only emissions that occur are the embedded emissions. Therefore, having lower embedded emissions, the

H2ICE hybrid buses have lower overall GHG emissions than fuel cell hybrid buses and conventional buses even having a lower efficiency.

4.4 Conclusions

Knowing that for air quality in big cities local emissions are the main concern and hydrogen fueled vehicles only emit indirect emissions, it is undoubted that the air quality of those cities would improve in every scenario. But as expected, the power generation source has a big impact on the well-to-wheel emissions of hydrogen vehicles. Assuming today's hydrogen production, 96% by SMR and 4% by electrolysis with the average carbon foot print of the Argentine grid, the GHG emissions of the hydrogen fueled bus models are lower than those of the CB.

The results also show the high potential of hydrogen fueled buses to reduce GHG emissions. However, if electrolysis with the average carbon foot print of the today's Argentine grid is used, the hydrogen fueled bus platforms have no greenhouse gas emission edge over CB. But assuming 2025's composition of power generation sources, the GHG emission reduction using electrolysis is higher than using a SMR. Scenario four has shown the potential of hydrogen fueled buses using renewable energy source in the production of electricity. Furthermore, scenario four has shown, looking at GHG emissions, that the efficiency becomes less important when the amount of renewable energy sources in the power generation production increase. Using 100% renewable energy sources, the efficiency benefit do not lead to benefits in the avoidance of GHG emissions.

In view of the fact that the efficiency do not has high impacts on the GHG emission avoidance of zero emission hybrid buses, the costs of the buses are an important factor. Therefore, the total cost of ownership and the cost of CO_2 avoided will be estimated in the following chapter.

Chapter 5

Financial Modeling

Throughout this chapter a financial modeling of the different bus platforms is done. The analysis includes the estimation of the purchase price of the different buses as well as the in-service costs, using the fuel consumption results of chapter three. The in-service costs are divided into fuel costs and maintenance costs.

5.1 Bus Purchase Price

To estimate the purchase price of the buses, these are subdivided into glider, power unit, electric drivetrain and hydrogen storage system. The electric drivetrain system includes the electric motor/generator and the power electronic, whereas the power unit consist either of an internal combustion engine or a fuel cell.

5.1.1 Glider

Due to higher security guidelines, extra space for fuel cell and tanks and a lower production volume, gliders prices of hydrogen fueled buses are significantly higher than those of conventional buses. According to a companies financial evaluation of operating Fuel Cell buses [5], the glider prices are shown in figure 5.1.

	CB	H2ICE-Li	H2ICE-ultracaps	FCHB-Li	FCHB-ultracaps
Glider	180,000	288,000	288,000	288,000	288,000

Table 5.1: Glider price for the different bus types in USD [5]

5.1.2 Engine and Fuel Cell Power Unit

Depending on the bus platform the power unit consists of a ICE, a H2ICE or a FC. Up on literature the price range for fuel cell systems is high. Upper prices according to researches are about USD 2,100 per kW [5], whereas the lower price according to a financial analysis of fuel cell systems [34] is USD 1,700 per kW. However, all the analysis's and researches are expecting a cost reduction for the near future [5]. Therefore, the lower price for fuel cell systems was used in this purchase price estimation. Gaseous fueled engines are already well developed and widely used.Therefore, the price of a H2ICE is comparable to that of a conventional ICE. Furthermore, according to fuel cell companies additional costs to connect the power unit with the electrical drivetrain accrue [5].

Table 5.2 shows the costs for the different powertrain systems according to the presented component costs and the bus specifications presented in the technical analysis.

	CB	H2ICE-Li	H2ICE-ultracaps	FCHB-Li	FCHB-ultracaps
Fuel Cell System	-	-	-	204,000	127,500
ICE	10,000	-	-	-	-
H2ICE	-	10,000	10,000	-	-
Build labour	-	10,000	10,000	14,000	14,000
Total Costs	10,000	20,000	20,000	218,000	141,500

Table 5.2: Power Unit Price of the different buses in USD [5, 8, 16, 34]

5.1.3 Hydrogen Storage System

As mentioned in the technical analysis, for the hydrogen storage system compressed hydrogen storage tanks are used. Compressed hydrogen storage tanks have already a market and today's costs for those tanks are USD 1,800 per kg hydrogen that can be stored [58]. Using this price assumption, the costs for the used storage tanks are established and are shown in table 5.3.

	CB	H2ICE-Li	H2ICE-ultracaps	FCHB-Li	FCHB-ultracaps
Storage tanks	-	63,000	63,000	63,000	56,000

Table 5.3: Hydrogen Storage System Price of the different buses in USD [5, 8, 16, 34]

5.1.4 Electric Storage System

For batteries prices between USD 500 per kWh and USD 1000 per kWh could be found in literature, whereas for ultracapacitors the prices are significantly higher and range between USD 9000 per kWh and USD 13,000 kWh [8, 34, 46]. According to this references, the price of USD 720 per kWh for Li-Batteries and USD 12,000 kWh for ultracapacitors is assumed to establish the electric storage system price. Ultracapacitors are not usual for mobile applications and therefore, a price which is located in the upper part of the price range is used. The price of the battery pack for each bus is shown in table 5.4

	CB	H2ICE-Li	H2ICE-ultracaps	FCHB-Li	FCHB-ultracaps
Battery Pack	-	30,300	36,000	19,500	24,000

Table 5.4: Electric Storage System Price of the different buses in USD [5, 8, 16, 34]

5.1.5 Electric Drivetrain System

The hybrid architecture proposed for the H2ICE buses includes an electric generator connected to the engine shaft which feeds the battery pack and/or the electric motor connected to the bus differential , whereas the drivetrain of the FCHB only includes one electric motor/generator[3]. Actual costs of an electric motor/generator are USD 40 per kW[34].

Based on the power requirements of the optimum configurations attained in Chapter 3 for the H2ICE hybrids and the vehicle specifications of the 2 evaluated FC buses, it is possible to determine the purchase cost of the pertinent systems. Results are shown in table 5.5.

Beside the motor/generator power electronics need to be included in the cost analysis. Available literature shows that these systems have an average value of between USD 30[34] and USD 50[5], therefore throughout this analysis an average value of USD 35 per KW will be used. The overall price of the different drive train systems are shown on Table 5.5

	CB	H2ICE-Li	H2ICE-ultracaps	FCHB-Li	FCHB-ultracaps
Electric drivetrain	-	7,200	7,200	9,600	5,400
Power electronic	-	6,300	6,300	8,400	4,700

Table 5.5: Electrical drivetrain costs for the different buses in USD[34]

5.1.6 Purchase Price

Based on the results presented above Figure 5.1.1 shows the overall cost of the different evaluated vehicles broken down into the different established components.

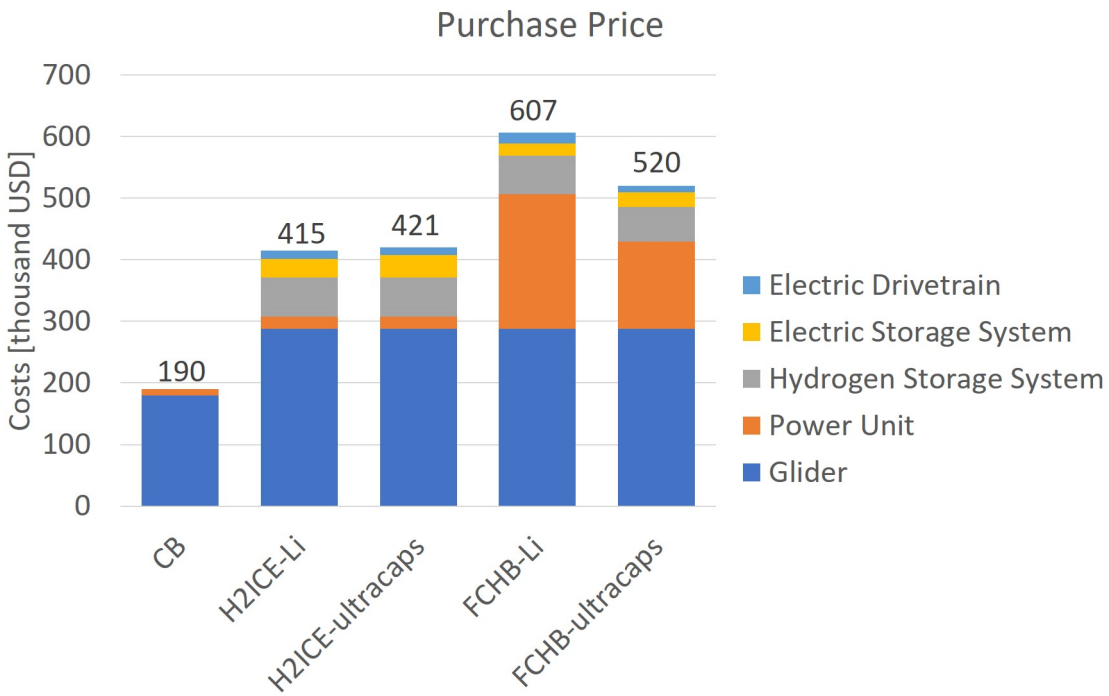

Figure 5.1.1: Purchase Price of the buses

As was expected, due to the battery pack which is included into the power system, the additional electric drivetrain, the additional hydrogen storage system and the higher glider costs, the H2ICE buses can not reach the low purchase price of a conventional bus. However, the H2ICE is a cheap alternative to the ICE compared to fuel cell systems as can be seen in figure 5.1.1 [34, 43].

5.2 In-Service Maintenance Costs

For the maintenance costs it is necessary to know if the battery pack has to be exchanged during the lifetime of the bus. Therefore, first of all the electric storage packs of the different buses were considered.

Energy Storage System

In Chapter 3.2.2 the ESS lifetime over the storage capacity was shown. For Li-Ion batteries a capacity of 42kWh is necessary to reach the bus lifetime of 10 years, whereas ultracapacitors only need a capacity of 3kWh to reach the bus lifetime [46].

With the electric storage capacity for the H2ICE established in the model optimization in chapter 3, the ESS endure the 10 years lifetime of the buses and do not have to be changed, whereas the ESS of the FC buses, according to the datasheet [11] do not endure the 10 years lifetime and have to be changed. Table 5.6 shows the calculated ESS costs.

	CB	H2ICE-Li	H2ICE-ultracaps	FCHB-Li	FCHB-ultracaps
Electr. Storage capacity [kWh]	-	42	3	27	2
Changes of the ESS	-	-	-	1	1
Costs [USD]	-	-	-	19,500	24,000

Table 5.6: Maintenance Costs of the ESS [34]

Maintenance Costs without ESS

The per year maintenance costs of the different buses are composed of electrical drivetrain maintenance and regular maintenance.

The electric drivetrain maintenance includes the maintenance of the electric motor/generator and the power electronic.

The regular maintenance includes the exchange of oil, wheels and the maintenance of the power unit. According to the literature the fuel cells need additionally one big maintenance through the 10 years and therefore the maintenance costs of the fuel cells are higher than those of ICE as can be seen in table 5.7 [5, 34].

	CB	H2ICE-Li	H2ICE-ultracaps	FCHB-Li	FCHB-ultracaps
Electr. Drivetrain	-	8,000	8,000	8,000	8,000
Regular Maintenance	14,500	14,500	14,500	40,000	35,000
Total Maintenance Costs	14,500	22,500	22,500	48,000	43,000

Table 5.7: Maintenance costs per year in USD without ESS[5, 34]

Because of that decrease in the current value of future cash flows, the Net Present Value (NPV) is used to calculate the present values of the future maintenance cash flows. For each erogation a NPV calculation was done based on an established discount rate and time of each payment. For the calculation an annual discount rate of 8% was used.

$$NPV = \sum_{t=1}^{T} \frac{C_t}{(1+r)^t},$$

with C_t =net cash inflow during the period t, r=discount rate and t = number of time periods. Table 5.8 shows the calculated maintenance costs in a lifetime of 10 years.

	CB	H2ICE-Li	H2ICE-ultracaps	FCHB-Li	FCHB-ultracaps
Maintenance Costs Lifetime [USD]	105,000	163,000	163,000	348,000	311,000

Table 5.8: Life time maintenance costs without ESS

Also, here the CB has the lowest costs because conventional buses do not need the maintenance of an electric drivetrain.

5.3 In-Service Fuel Costs

Using the fuel consumption results established in Chapter 3 (Figure 3.2.2), the specific cost of the different fuels and assuming that a bus does 220 km per day for 10 years, the NPV of the fuel used over the life time of the bus can be calculated for the different technologies.

The average price of grade 3 diesel (>10pmm of sulphur) used in the current Euro V buses is USD 1.2 per liter [46].

Today's hydrogen price ranges between USD 6 per kg and USD 4 per kg. Therefore, USD 5 per kg can be assumed as an accurate hydrogen price for the next years [5, 43]. Therefore, using these fuel costs and the same annual discount rate as that used for the maintenance costs, it is possible to establish the lifetime fuel costs of the different evaluated buses. Results are shown in Table 5.9.

	CB	H2ICE-Li	H2ICE-ultracaps	FCHB-Li	FCHB-ultracaps
Fuel costs [USD]	365,000	310,000	320,000	280,000	295,000

Table 5.9: In-Service Fuel costs over a 10 year lifetime

Having a lower fuel consumption the fuel cell hybrid bus models can reach the lowest fuel costs of all the evaluated bus platforms. But also the H2ICE hybrid can reach about 15% lower fuel costs than the CB model. However, due to their about 10% lower efficiency, the fuel costs of the H2ICE are 10% higher than those of the fuel cell buses.

5.4 Total Cost of Ownership

The total cost of ownership (TCO) of the different evaluated buses can be calculated as the sum of the NPV of the different costs depicted throughout this chapter. These are shown on Figure 5.4.1.

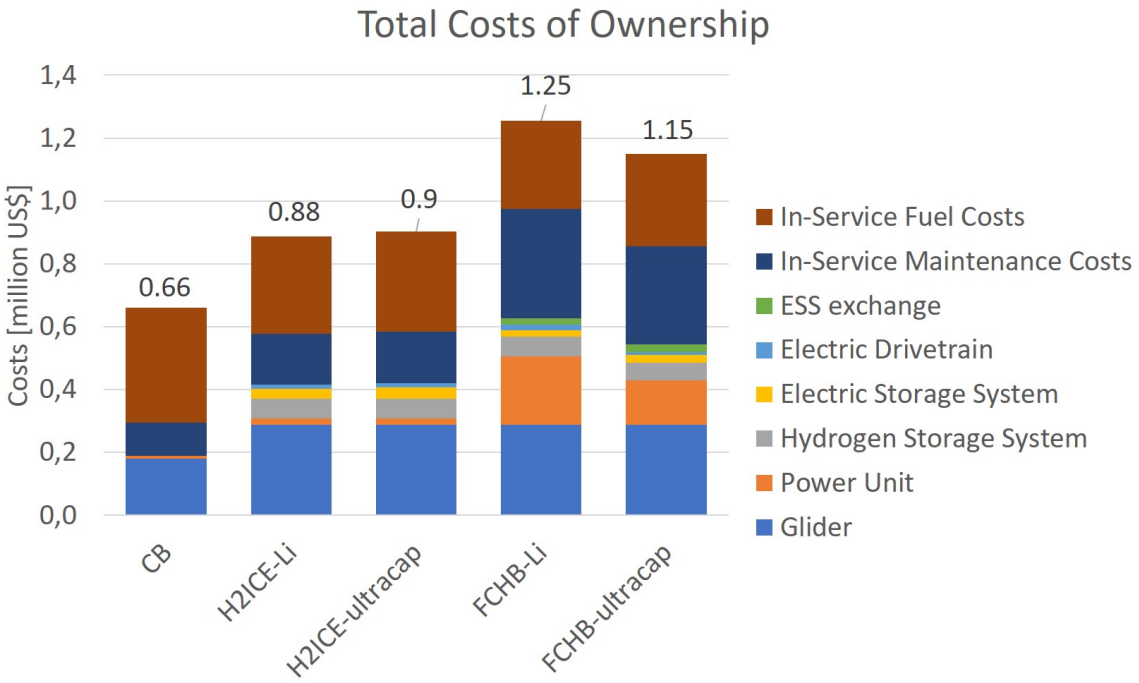

Figure 5.4.1: Total Costs of Ownership

Due to the higher bus part costs such as for the glider, the additional electric drivetrain, the hydrogen storage system and the electric storage system, as well as the higher maintenance costs the hydrogen fueled buses prices are appreciably higher than those of conventional buses. Furthermore, higher costs of hydrogen result in fuel costs almost as high as those of conventional buses even having a significant lower fuel consumption. However, compared to the Fuel Cell buses the H2ICE hybrid buses can reach much lower total costs of ownership. This is

mainly because of the low costs of the ICE and the low maintenance costs of the ICE compared to the costs of fuel cells and fuel cell maintenance.

5.5 Cost of CO_2 avoided

With the total costs of ownership of the different bus platforms and the calculated GHG emissions the cost of CO_2 eq. avoided can be calculated. To estimate the cost of CO_2avoided the higher costs of the hybrid buses are divided trough the avoided GHG emissions by applying the following formula:

$$\text{Cost of } CO_2\text{avoided} = \frac{(HB_{PP} - CB_{PP})}{(CB_{GHG} - HB_{GHG})},$$

with HB_{PP} =Hybrid Bus Purchase Price, CB_{PP} =Conventional Bus Purchase Price, HB_{GHG} =Hybrid Bus GHG Emissions, CB_{GHG} =Conventional Bus GHG Emissions

The calculation was done for all four scenarios. However, producing more GHG emissions and having higher total costs of ownership for all hydrogen fueled buses in the second scenario, the calculation of CO_2 eq. avoided does not make any sense. Therefore, figure 5.5.1 shows only the cost of CO_2 eq. avoided for the first, second and fourth scenario.

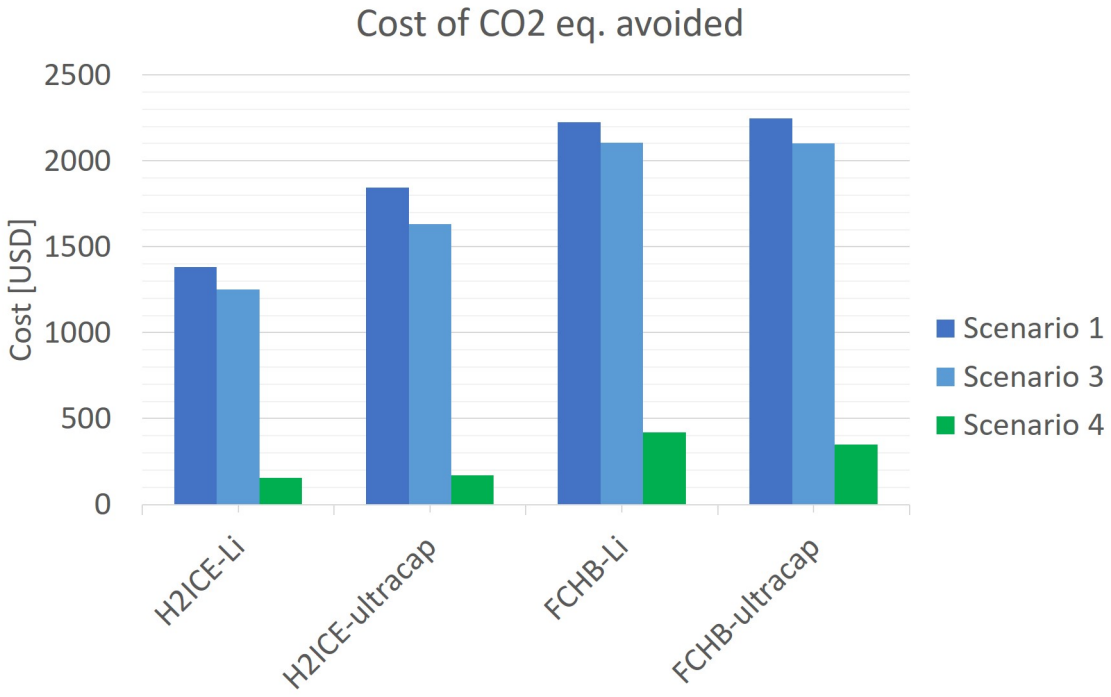

Figure 5.5.1: Costs in US$ per saved ton of global greenhouse gases

Due to the much lower total cost of ownership of the H2ICE hybrid buses, they have benefits over the fuel cell buses in all four scenarios. Scenario one shows that using natural gas in the production process of hydrogen the cost of CO_2 eq. avoided is with USD 1200 to USD 2200 very high. However, it also can be seen that, using electrolysis, the impact of the amount of renewable energies in the production of electricity is enormous. The figure shows, using electrolysis, about 55% of the power generation sources have to be almost emission free to reach the cost of CO_2 eq. avoided from scenario one. But using 100% renewable energies in the power generation process, the cost of CO_2 eq. avoided can be decreased to USD 200 per ton CO_2 eq..

5.6 Conclusion

The financial analysis shows that no hydrogen fueled hybrid bus reaches the low costs of a conventional diesel bus. The fact that an extra electric drive train is necessary and that the maintenance costs of the hydrogen fueled buses are higher results in higher overall ownership costs. Among the hydrogen fueled buses the FCHB have a higher costs because the fuel cell is still a costly application. The FCHB-Li has the highest ownership costs because of its high fuel cell power.

With a look at the costs for the reduction of the GHG emissions the H2ICE buses can outperform the FCHB. Assuming hydrogen produced by SMR, what is today's most common production method, the cost of CO_2 eq. avoided are with a FCHB significantly higher than with a H2ICE bus.

Chapter 6

Conclusion

The provision of the technical, environmental and financial analysis has shown that the H2ICE hybrid bus has some benefits compared to fuel cell buses and other conventional bus alternatives.

By using any hybrid powertrain architecture, the fuel consumption can be reduced significantly. The study showed that the H2ICE hybrid bus can almost reach the low consumption of Fuel-Cell hybrid buses, but having an about 10% lower efficiency.

The global GHG emissions can be reduced dramatically using SMR as production method of hydrogen, whereas using electrolysis at least 45% of the electricity has to come from zero emission power generations to reach the levels of produced GHG emissions using SMR. Furthermore, rising the amount of renewable energies the emissions can be reduced even more and the analysis has shown that the lower efficiency of the H2ICE has no impact on the GHG emissions if the power generation processes are using 100% renewable energies. Because the combustion of hydrogen do not produce any emissions and therefore the direct emissions are almost zero, the positive influence on air and life in the city is big. Looking at the embedded emissions the H2ICE hybrid bus can reach almost the levels of conventional buses and has big advantages over fuel cell buses. Furthermore, the well known ICE can assure the high reliability that is needed in public transportation.

As presumed, none of the hydrogen fueled buses can reach the low costs of ownership of conventional buses. However, because of the low cost ICE, the H2ICE bus outperforms the fuel cell bus strongly and moves the H2ICE bus purchase price close to the purchase price of conventional buses. Due to the lower purchase price, the cost of CO_2 eq. avoided can be reduced by over 60%, compared to fuel cell hybrid buses. Therefore, the H2ICE hybrid bus is a low cost alternative to other zero direct emission buses and especially interesting for developing countries to improve the air quality in big cities.

Bibliography

[1] James A. Adams, Woong chul Yang, Keith A. Oglesby, and Kurt D. Osborne. The Development of Ford's P2000 Fuel Cell Vehicle. In *SAE Technical Paper Series*. SAE International, mar 2000. doi: 10.4271/2000-01-1061.

[2] Rajesh K. Ahluwalia, X. Wang, and A. Rousseau. Fuel economy of hybrid fuel-cell vehicles. *Journal of Power Sources*, 152:233–244, dec 2005. doi: 10.1016/j.jpowsour.2005.01.052.

[3] Argonne. Autonomie. Modelling and Simulation Program.

[4] J. Bauman and M. Kazerani. A Comparative Study of Fuel-Cell–Battery, Fuel-Cell–Ultracapacitor, and Fuel-Cell–Battery–Ultracapacitor Vehicles. *IEEE Transactions on Vehicular Technology*, 57(2):760–769, mar 2008. doi: 10.1109/tvt.2007.906379.

[5] Edward Boyd Ben Madden. Economic Case for Hydrogen Buses in Europa. Technical report, Ballard, 2017.

[6] Mercedes Benz. Conventional Bus MB Data. Technical report, MerBenzData.

[7] Roland Berger. Fuel Cell Electric Buses - Potential for Sustainable Public Transport in Europe. Technical report, The Fuel Cells and Hydrogen Joint Undertaking, 2015.

[8] Aaron Brooker, Matthew Thornton, and John Rugh. Technology Improvement Pathways to Cost-effective Vehicle Electrification. In *SAE Technical Paper Series*. SAE International, apr 2010. doi: 10.4271/2010-01-0824.

[9] Maryyeh Chehresaz. *Modeling and Design Optimization of Plug-In Hybrid Electric Vehicle Powertrains*. PhD thesis, University of Waterloo, 2013.

[10] CHIC. Clean Hydrogen in European Cities: Key Facts, Results,Recommendations. Technical report, CHIC, 2016.

[11] Ch. Chilev and F. Darkrim Lamari. Hydrogen storage at low temperature and high pressure for application in automobile manufacturing. *International Journal of Hydrogen Energy*, 41(3):1744–1758, jan 2016. doi: 10.1016/j.ijhydene.2015.11.099.

[12] Ministerio de Energia y Mineria. Informe Trimestral de Coyuntura Energetica. Technical report, Ministerio de Energia y Mineria, 2018.

[13] Miniterio de Energia y Mineria. Energy Scenarios 2025. Technical report, Miniterio de Energia y Mineria, 2016.

[14] Ministerio de EnergÃa y MinerÃa. Balance EnergÃ©tico Nacional 2016. Technical report, Ministerio de EnergÃa y MinerÃa, Gobierno de Argentina, 2017.

[15] Asociacion de Fabricas Argentinas de Componentes. Flota circulante en Argentina 2016. Technical report, Asociacion de Fabricas Argentinas de Componentes, 2017.

[16] N. de Miguel, R. Ortiz Cebolla, B. Acosta, P. Moretto, F. Harskamp, and C. Bonato. Compressed hydrogen tanks for on-board application: Thermal behaviour during cycling. *International Journal of Hydrogen Energy*, 40(19):6449–6458, may 2015. doi: 10.1016/j.ijhydene.2015.03.035.

[17] Vipin Dhyani and K. A. Subramanian. Experimental investigation on effects of knocking on backfire and its control in a hydrogen fueled spark ignition engine. *International Journal of Hydrogen Energy*, 43(14):7169–7178, apr 2018. doi: 10.1016/j.ijhydene.2018.02.125.

[18] Prof. Dr. Martin Doppelbauer. Hybrids and electrical Vehicles. Lecture Notes, 2018.

[19] Amgad Elgowainy, Andrew Burnham, Michael Wang, John Molburg, and Aymeric Rousseau. Well-To-Wheels Energy Use and Greenhouse Gas Emissions of Plug-in Hybrid Electric Vehicles. *SAE International Journal of Fuels and Lubricants*, 2(1):627–644, apr 2009. doi: 10.4271/2009-01-1309.

[20] Nicolaos Lymberopoulos Christodoulos N. Christodoulou Emmanuel Zoulias, Elli Varkaraki and George N. Karagiorgis. A Review on Water Electrolysis. Technical report, Centre for Renewable Energy Sources (CRES), Frederick Research Center (FRC), 2002.

[21] Tom Fletcher, Rob Thring, and Martin Watkinson. An Energy Management Strategy to concurrently optimise fuel consumption & PEM fuel cell lifetime in a hybrid vehicle.

International Journal of Hydrogen Energy, 41(46):21503–21515, dec 2016. doi: 10.1016/j.ijhydene.2016.08.157.

[22] Chao Fu, Rahul Anantharaman, Kristin Jordal, and Truls Gundersen. Thermal efficiency of coal-fired power plants: From theoretical to practical assessments. *Energy Conversion and Management*, 105:530–544, nov 2015. doi: 10.1016/j.enconman.2015.08.019.

[23] Evangelos G. Giakoumis. *Driving and Engine Cycles*. Springer International Publishing, 2017. doi: 10.1007/978-3-319-49034-2.

[24] John Heywood. *Internal Combustion Engine Fundamentals*. McGraw-Hill Education, 1988. ISBN 0-07-028637-x. URL https://www.amazon.com/Internal-Combustion-Engine-Fundamentals-Heywood/dp/007028637X?SubscriptionId=0JYN1NVW651KCA56C102&tag=techkie-20&linkCode=xm2&camp=2025&creative=165953&creativeASIN=007028637X.

[25] Thanh Hua, Rajesh Ahluwalia, J. K. Peng, Matt Kromer, Stephen Lasher, Kurtis McKenney, Karen Law, and Jayanti Sinha. Technical Assessment of Compressed Hydrogen Storage Tank Systems for Automotive Applications. Technical report, Argonne National Laboratory, sep 2010.

[26] Thanh Hua, Rajesh Ahluwalia, Leslie Eudy, Gregg Singer, Boris Jermer, Nick Asselin-Miller, Silvia Wessel, Timothy Patterson, and Jason Marcinkoski. Status of hydrogen fuel cell electric buses worldwide. *Journal of Power Sources*, 269:975–993, dec 2014. doi: 10.1016/j.jpowsour.2014.06.055.

[27] IPCC. Greenhouse Gas Protocol. 2017.

[28] Frank E. Belles Isadore L. Drell. Survey of Hydrogen Combustion Properties. Technical report, Lewis Flight Propulsion Laboratory.

[29] Sergio Junco, Pedro Orbaiz, Norberto M. Nigro, and Mauro G. Carignano. Hybridisation effect on operating costs and optimal sizing of components for hybrid electric vehicles. *International Journal of Simulation and Process Modelling*, 12(3/4):221, 2017. doi: 10.1504/ijspm.2017.10006527.

[30] Alireza Khaligh and Zhihao Li. Battery, Ultracapacitor, Fuel Cell, and Hybrid Energy Storage Systems for Electric, Hybrid Electric, Fuel Cell, and Plug-In Hybrid Electric Vehicles: State of the Art. *IEEE Transactions on Vehicular Technology*, 59(6):2806–2814, jul 2010. doi: 10.1109/tvt.2010.2047877.

[31] Min-Joong Kim and Huei Peng. Power management and design optimization of fuel cell/battery hybrid vehicles. *Journal of Power Sources*, 165(2):819–832, mar 2007. doi: 10.1016/j.jpowsour.2006.12.038.

[32] Manfred Klell, Helmut Eichlseder, and Alexander Trattner. *Wasserstoff in der Fahrzeugtechnik*. Springer Fachmedien Wiesbaden, 2018. URL https://www.ebook.de/de/product/32461883/manfred_klell_helmut_eichlseder_alexander_trattner_wasserstoff_in_der_fahrzeugtechnik.html.

[33] Thomas Koch. Verbrennungsmotoren 1. Lecture notes, 2017.

[34] Robert Kochhan, Stephan Fuchs andBenjamin Reuter, Peter Burda, Stephan Matz, and Markus Lienkamp. An Overview of Costs for Vehicle Components, Fuels and Greenhouse Gas Emissions. Technical report, Institute of Automotive Technology Technische UniversitÃ€t MÃŒnchen, TUM CREATE Limited, 2014.

[35] Peter Kurzweil. *Brennstoffzellentechnik: Grundlagen, Komponenten, Systeme, Anwendungen (German Edition)*. Springer Vieweg, 2012. ISBN 978-3-658-00084-4. URL https://www.amazon.com/Brennstoffzellentechnik-Grundlagen-Komponenten-Systeme-Anwendungen/dp/3658000848?SubscriptionId=AKIAIOBINVZYXZQZ2U3A&tag=chimbori05-20&linkCode=xm2&camp=2025&creative=165953&creativeASIN=3658000848.

[36] A. R. G. O. N. N. E. N. A. T. I. O. N. A. L. LABORATORY. GREET1 MODEL. Technical report, ARGONNE NATIONAL LABORATORY, 2012.

[37] A. R. G. O. N. N. E. N. A. T. I. O. N. A. L. LABORATORY. GREET2 MODEL. Technical report, ARGONNE NATIONAL LABORATORY, 2012.

[38] Antti Lajunen and Timothy Lipman. Lifecycle cost assessment and carbon dioxide emissions of diesel, natural gas, hybrid electric, fuel cell hybrid and electric transit buses. *Energy*, 106:329–342, jul 2016. doi: 10.1016/j.energy.2016.03.075.

[39] E. Laura, A. Nicolas, and Andrea L. Pineda Rojas. Evaluation of an Emission Inventory and Air Pollution in the Metropolitan Area of Buenos Aires. In *Air Quality-Models and Applications*. InTech, jun 2011. doi: 10.5772/18767.

[40] Moataz Mahmoud, Ryan Garnett, Mark Ferguson, and Pavlos Kanaroglou. Electric buses: A review of alternative powertrains. *Renewable and Sustainable Energy Reviews*, 62:673–684, sep 2016. doi: 10.1016/j.rser.2016.05.019.

[41] Kerstin K. MÃŒller. Final Report, Part A - Final Publishable Summary Report. Technical report, Clean Hydrogen in European Cities, 2016.

[42] G. Napoli, S. Micari, G. Dispenza, S. Di Novo, V. Antonucci, and L. Andaloro. Development of a fuel cell hybrid electric powertrain: A real case study on a Minibus application. *International Journal of Hydrogen Energy*, 42(46):28034–28047, nov 2017. doi: 10.1016/j.ijhydene.2017.07.239.

[43] Catharine Reid Nicolas Pocard. Fuel Cell Electric Buses An attractive value proposition for zero-emission busses in the United Kingdom. Technical report, Ballard Power Systems Inc., 2016.

[44] Nils-Olof Nylund, Kimmo ErkkilÃ€, Nigel Clark, and Greg Rideout. Evaluation of duty cycles for heavyduty urban vehicles, Final report of IEA AMF Annex XXIX. Technical report, VTT Technical REsearch Centre of Finland, 2007.

[45] Pedro Orbaiz. Hydrogen Characteristics. Lecture Notes, 2017.

[46] Pedro Orbaiz, Nicolás van Dijk, Santiago Cosentino, Nicolas Oxenford, Mauro Carignano, and Norberto Marcelo Nigro. A Technical, Environmental and Financial Analysis of Hybrid Buses Used for Public Transport. In *SAE Technical Paper Series*. SAE International, apr 2018. doi: 10.4271/2018-01-0424.

[47] Pedro JosÃ© Orbaiz. *Hybrid Chemical Recuperation of Spark Ignited Natural Gas Internal Combustion Engine*. PhD thesis, The University of Melbourne - Department of Mechanical Engineering, September 2012.

[48] Hannah Ritchie and Max Roser. CO2 and other Greenhouse Gas Emissions. Technical report, Our world in Data, 2018.

[49] M. ROSEN. Thermodynamic comparison of hydrogen production processes. *International Journal of Hydrogen Energy*, 21(5):349–365, may 1996. doi: 10.1016/0360-3199(95)00090-9.

[50] A. Rousseau, P. Sharer, and R. Ahluwalia. Energy Storage Requirements for Fuel Cell Vehicles. In *SAE Technical Paper Series*. SAE International, mar 2004. doi: 10.4271/2004-01-1302.

[51] Adrian Schneuwly. Energy Storage for Hybrid Power in Heavy Transportation. Technical report, Maxwell Technologies SA, 2009.

[52] Sebastian Verhelst and Thomas Wallner. Hydrogen-fueled internal combustion engines. *Progress in Energy and Combustion Science*, 35(6):490–527, dec 2009. doi: 10.1016/j.pecs.2009.08.001.

[53] Sebastian Verhelst, Roger Sierens, and Stefaan Verstraeten. A Critical Review of Experimental Research on Hydrogen Fueled SI Engines. In *SAE Technical Paper Series*. SAE International, apr 2006. doi: 10.4271/2006-01-0430.

[54] C. WHITE, R. STEEPER, and A. L. U. T. Z. The hydrogen-fueled internal combustion engine: a technical review. *International Journal of Hydrogen Energy*, 31(10):1292–1305, aug 2006. doi: 10.1016/j.ijhydene.2005.12.001.

[55] Ye Wu, Michael Q. Wang, Phillip B. Sharer, and Aymeric Rousseau. Well-to-Wheels Results of Energy Use, Greenhouse Gas Emissions, and Criteria Air Pollutant Emissions of Selected Vehicle/Fuel Systems. In *SAE Technical Paper Series*. SAE International, apr 2006. doi: 10.4271/2006-01-0377.

[56] Zhixin Wu, Michael Wang, Jihu Zheng, Xin Sun, Mingnan Zhao, and Xue Wang. Life cycle greenhouse gas emission reduction potential of battery electric vehicle. *Journal of Cleaner Production*, 190:462–470, jul 2018. doi: 10.1016/j.jclepro.2018.04.036.

[57] Bolun Xu, Alexandre Oudalov, Andreas Ulbig, Goran Andersson, and Daniel S. Kirschen. Modeling of Lithium-Ion Battery Degradation for Cell Life Assessment. *IEEE Transactions on Smart Grid*, 9(2):1131–1140, mar 2018. doi: 10.1109/tsg.2016.2578950.

[58] Jinyang Zheng, Xianxin Liu, Ping Xu, Pengfei Liu, Yongzhi Zhao, and Jian Yang. Development of high pressure gaseous hydrogen storage technologies. *International Journal of Hydrogen Energy*, 37(1):1048–1057, jan 2012. doi: 10.1016/j.ijhydene.2011.02.125.